(2)

May 1991

DCIEM No. 91-45

METHODOLOGY FOR CALIBRATION AND USE OF HEAT FLUX TRANSDUCERS

M.B. Ducharme
J. Frim

Defence and Civil Institute of Environmental Medicine
1133 Sheppard Avenue West
P.O. Box 2000
North York, Ontario
M3M 3B9

Department of National Defence - Canada

TABLE OF CONTENTS

LIST OF ABBREVIATIONS

$\dot{H}$: Heat flux ($W \cdot m^{-2}$)
$\dot{H}_{corr}$: Heat flux corrected for the insulating effect of the HFT ($W \cdot m^{-2}$)
$\dot{H}_{meas}$: Measured heat flux ($W \cdot m^{-2}$)
$\dot{H}_{Rapid\text{-}k}$: Heat flux through the Rapid-k heat flow meter ($W \cdot m^{-2}$)
k : Thermal conductivity ($W \cdot °C^{-1} \cdot m^{-1}$)
R : Thermal resistance ($°C \cdot m^2 \cdot W^{-1}$)
R_m : Thermal resistance of the variable-R model ($°C \cdot m^2 \cdot W^{-1}$)
R_t : Thermal resistance of tissue ($°C \cdot m^2 \cdot W^{-1}$)
R_T : Thermal resistance of HFT ($°C \cdot m^2 \cdot W^{-1}$)
R_w : Thermal resistance of water ($°C \cdot m^2 \cdot W^{-1}$)
T : Temperature (°C)
ΔT : Temperature difference (°C)
T_c : Core temperature of the body segment (°C)
T_{cold} : Surface temperature of the cold plate of the Rapid-k (°C)
T_{hot} : Surface temperature of the hot plate of the Rapid-k (°C)
T_l : Temperature of the lower surface of the HFT (°C)
T_m : Muscle temperature (°C)
T_{sk} : Skin temperature (°C)
T_u : Temperature of the upper surface of the HFT (°C)
T_w : Temperature of the water (°C)
V : Voltage (mV)
x : Thickness (m)

ABSTRACT

The direct assessment of heat flux from the body is a basic measurement in thermal physiology. Heat flux transducers (HFTs) are being used increasingly for that purpose under different environmental conditions. However, questions have been raised regarding the accuracy of the manufacturer's constant of calibration, and also about the effect of the thermal resistance of the device on the true thermal flux from the skin. Two different types of waterproofed HFTs were checked for their calibration using the Rapid-k thermal conductivity instrument. A detailed description of the methodology used during the calibration is given. The mean differences between our calibration constants and the manufacturers' constants were +20.2 ± 7.1% ($n = 15$) for Thermonetics Corporation's HFTs (San Diego, CA) and -0.7 + 4.8% ($n = 12$) for Concept Engineering's HFTs (Old Saybrook, CT). The highly significant statistical difference in the error of calibration between the two manufacturers ($p < 0.001$) becomes an important criterion for the selection of HFTs.

A model capable of simulating a large range of "tissue" insulation was used to study the effect of the underlying tissue insulation on the relative error in thermal flux due to the thermal resistance of the HFTs. The data show that the deviation from the true value of thermal flux increases with the reciprocal of the underlying tissue insulation ($r = 0.99$, $p < 0.001$). The underestimation of the heat flux through the skin measured by an HFT is minimal when the device is used on vasoconstricted skin in cool subjects (3 to 13% error), but becomes important when used on warm vasodilated subjects (29 to 35% error), and even more important on metallic skin mannequins (> 60% error). In order to optimize the accuracy of the heat flux measurements by HFTs, it is important to recalibrate the HFTs from Thermonetics Corporation, and to correct the heat flux values for the thermal resistance of the HFT when used on vasodilated tissues.

1. INTRODUCTION

The direct assessment of heat flux from the body is a basic measurement in thermal physiology. Heat flux transducers (HFTs) are being used increasingly for this purpose in preference to calorimeters because of their reduced cost, their ease of application and their capability to be used under different and often more realistic environmental conditions.

A HFT consists of a sensitive thermopile composed of many fine-gauge thermocouples connected in series on opposite sides of a flat matrix with a stable thermal resistance (see Fig. 1). This thermal resistance R_T creates a temperature difference ΔT across the matrix in the presence of heat flux $\dot{H}$:

$$\Delta T = R_T \cdot \dot{H}. \quad (1)$$

The temperature difference is detected by the thermocouple junctions, and the voltage generated across the thermopile is proportional to the heat flux through the HFT. The sensitivity of the device ($mV \cdot m^2 \cdot W^{-1}$) is proportional to the number of thermocouple junctions in series and to the thermal resistance R_T of the matrix.

Despite the simplicity of the design, questions have been raised regarding the reliability and accuracy of HFTs. Nuckols and Piantadosi (7) developed a calibration technique for HFTs and showed an effect of temperature on the performance of the HFTs, as well as significant differences of up to 20% between the factory-supplied calibration constants (using HFTs from Thermonetics Corporation) and those determined experimentally. The authors concluded that potentially large errors in calculated convective heat flow may arise if transducers are not accurately calibrated. They suggested that HFTs should be carefully recalibrated to avoid this error.

Recently, Sowood (12), using a similar method of calibration, showed that the experimentally determined calibration constants of HFTs were the same as those of the manufacturer (using HFTs from Concept Engineering) minus approximately 6 $W \cdot m^{-2} \cdot mV^{-1}$. He concluded that the differences between the two sets of values were negligible and that the devices could be used without recalibration.

These two studies raise questions regarding a potential difference in the accuracy of HFT calibrations between manufacturers. If such a difference is demonstrable when using a single reliable method of calibration for both types of HFTs, the implication could be important in the selection of HFTs by those who do not have access to calibration facilities.

Poppendick (8), Gin et al. (6), and later Wissler and Ketch (14) observed another potential source of error involved in the use of HFTs. The design of the HFT involves compromise. The

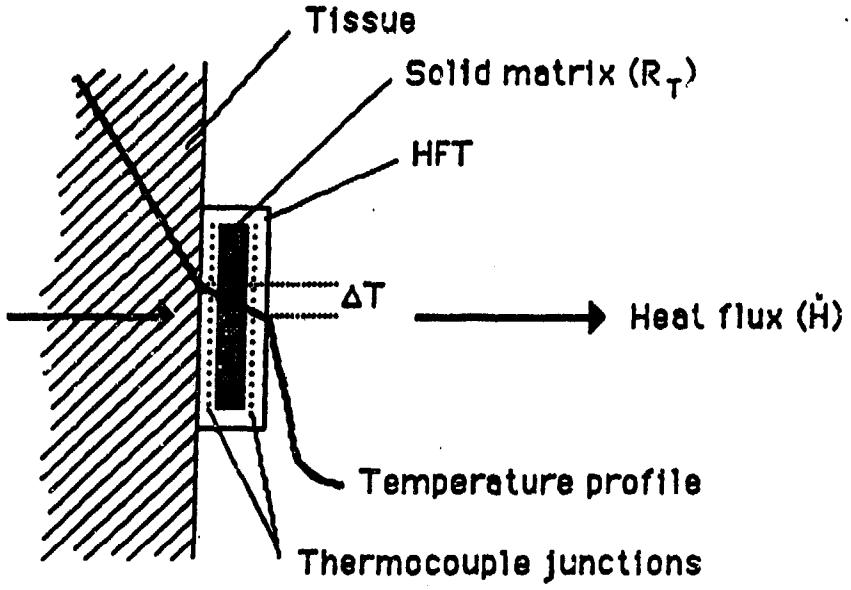

Figure 1: Temperature profile through a biological heat transfer system including a heat flux transducer.

addition of the thermal resistance R_T of the HFT on the surface under study will modify the insulation of the region and consequently change the skin temperature and heat flux. When an HFT is used on the skin in water, where the thermal resistance between the skin surface and the environment is small, a significant local increase in thermal resistance may occur. Therefore, the voltage obtained from the HFT is only representative of the heat flow from the tissue immediately below the disc, not that of the adjacent areas of exposed skin. Wissler and Ketch (14) calculated in their study that when used in water, the HFT can underestimate the thermal flux by 15 to 20% because of the thermal resistance of the transducer. In addition, Gin et al. (6) suggested that the error could be greater when HFTs are used on vasodilated skin. Despite the suggestion that the magnitude of the error might be related to the vascular state of the underlying tissue, no information is available in the literature about the relationship between the error in heat flux values due to the resistance of HFTs and the underlying tissue insulation.

This study presents a detailed description of the methodology used for calibrating HFTs. The recalibration of HFTs from two companies (Thermonetics Corporation and Concept Engineering) is presented and recommendations are given related to the selection and use of HFTs. In addition, the study gives new evidence for the importance of correcting the thermal flux values for the thermal resistance of the HFT when used under certain conditions. The latter information has been published in condensed form in the open literature (5).

2. MATERIAL AND METHODS

2.1 Calibration of the Rapid-k instrument

2.1.1 The Rapid-k instrument

The Rapid-k instrument (Dynatech R/D Company, Mass) is an apparatus designed to determine the thermal conductivity of materials in accordance with ASTM C518 "Specifications for the Measurement of Thermal Conductivity by Means of the Heat Flow Meter". When calibrated properly, it can operate as a reference instrument for the calibration of HFTs.

Heat flow through a solid results from having a temperature gradient in the material. The thermal conductivity is a material property which determines how much heat flows through a given thickness of the material when submitted to a temperature difference. The Fourier linear heat flow equation defines thermal conductivity under steady state conditions as:

$$k = \frac{\dot{H} \cdot x}{\Delta T} \qquad (2)$$

where k is the thermal conductivity of the material in $W \cdot °C^{-1} \cdot m^{-1}$, $\dot{H}$ is the heat flux through the material in $W \cdot m^{-2}$, x is the thickness of the material under investigation, and ΔT is the temperature difference between the two opposite surfaces of the material in °C.

The determination of thermal conductivity using the Rapid-k instrument is made by placing a sample of the material (30 cm wide x 30 cm long x 2 to 5 cm thick) between two copper plates which are maintained at known temperatures. Because of the temperature difference between the surfaces, heat will flow through the sample from the hot side to the cold side (see Fig. 2A). The quantity of heat flowing through the sample is measured by a very sensitive heat flow meter located between the sample and the cold plate (the term "meter" is used in reference to the internal HFT of the Rapid-k to avoid confusion with the HFT under test). The heat flow through the central 10 cm x 10 cm area of the sample, called the effective area, is unidirectional and uniform between the hot and the cold plate.

If the k value of the sample is known, the value of $\dot{H}$ can be calculated knowing x and ΔT. The relationship between the voltage output of the heat flow meter and $\dot{H}$ can be determined by applying different ΔTs to the copper plates. This is the basic principle of the Rapid-k calibration.

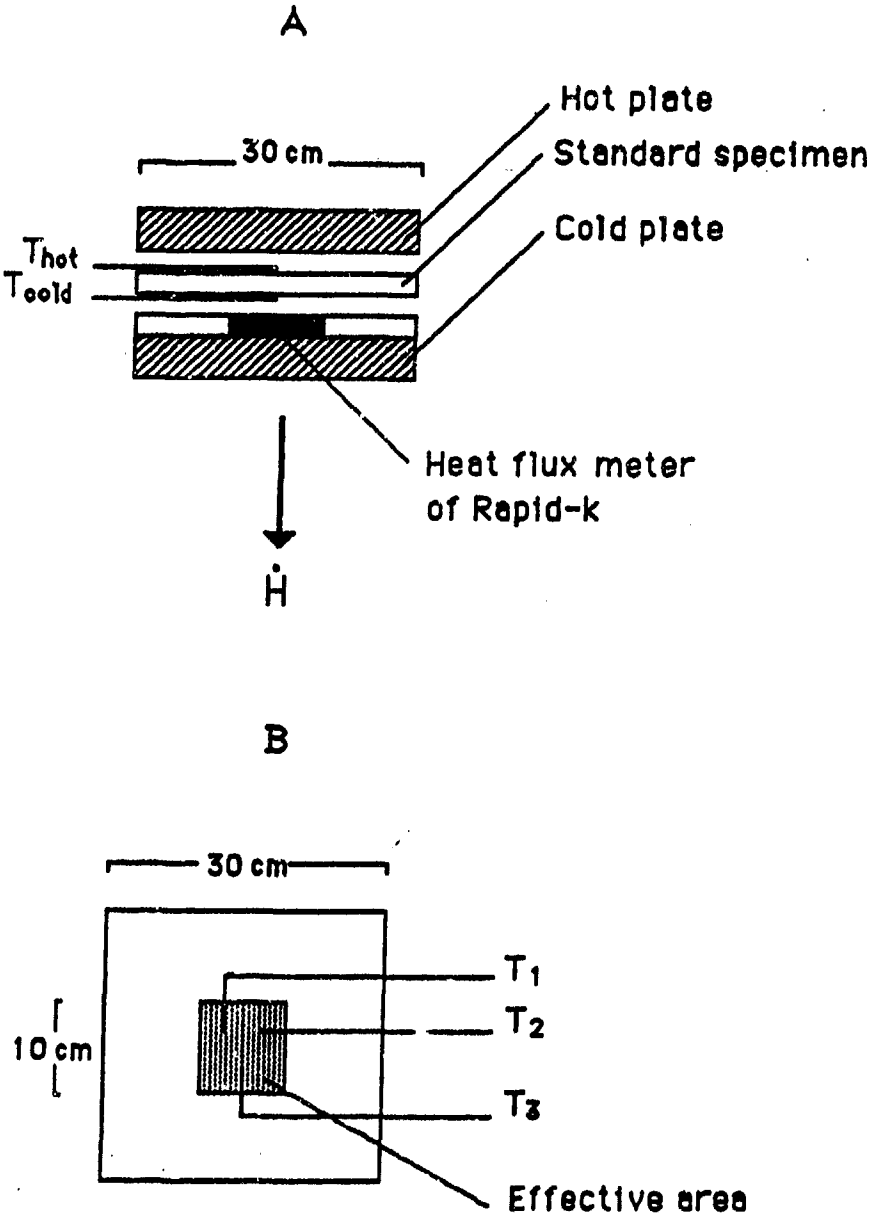

Figure 2: Cross-sectional (A) and top (B) views of the Rapid-k test set-up and placement of the thermocouples for the measurement of ΔT between the two opposite plate surfaces of the thermal resistance standard. The thermocouple junctions are fixed inside the effective area where the value $\dot{H}$ is measured by the heat flow meter of the Rapid-k. The gaps between the plates and the standard on A are present only for the clarity of the figure.

To ensure optimal performance of the Rapid-k, the heat flow meter of the instrument must be calibrated against a thermal resistance standard. For that purpose, two thermal resistance standard specimens were borrowed from the Thermal Performance Section of the National Research Council of Canada (NRC).

2.1.2 The National Research Council thermal resistance standards

Table 1 presents the calibration data provided for the standards (MDGB Transfer Standards #357-172-A,B) by NRC. The two calibrated standard specimens had identical calibrations:

$$R = (0.882581 \pm 1.40447E\text{-}03) - (2.87934E\text{-}03 \pm 5.34837E\text{-}05) \cdot T \quad (3)$$

where R is the thermal resistance of the standard in $°C \cdot m^2 \cdot W^{-1}$, and T is the mean temperature of the standard in °C. The thicknesses of the acrylic framed standards were 26.03 mm for specimen A and 26.01 mm for specimen B.

2.1.3 Rapid-k calibration

This calibration intended to establish the relationship between the heat flow meter output of the Rapid-k (V, in mV) and the calculated heat flux ($\dot{H}$ in $W \cdot m^{-2}$) using the standard resistance specimen of known thermal resistance (R in $°C \cdot m^2 \cdot W^{-1}$). The following equations were used to calculate the heat flux through the standard when exposed to a temperature difference ΔT:

$$\dot{H} = R \cdot \Delta T \quad (4)$$

or

$$\dot{H} = (0.882581\text{-}2.87934E\text{-}03 \cdot T) \cdot (T_{hot} - T_{cold}) \quad (5)$$

where T is the mean temperature of the standard. The temperature difference ΔT was measured accurately with six fine gauge thermocouples (AWG 40) calibrated against a quartz thermometer (HP 2804A) to an accuracy of 0.07°C in a well-stirred temperature controlled water bath between 5 and 80°C. Preliminary experiments have shown that by using the thermocouples embedded in the copper plates of the Rapid-k to measure the ΔT, an error of approximately 4% is introduced in the calculation of $\dot{H}$. Three thermocouples were fixed on each surface of the standard within the 10 cm x 10 cm effective area where the heat flow meter of the Rapid-k is located (see Fig. 2B). The mean temperature of the specimen was calculated from the mean value of the six thermocouple readings.

Table 1: Thermal resistance data provided by the National Research Council for the MDGF Transfer Standards #357-172-A,B.

Mean temperature of standard (°C)	Measured thermal resistance ($^\circ C \cdot m^2 \cdot W^{-1}$)	Calculated thermal resistance ($^\circ C \cdot m^2 \cdot W^{-1}$)	Difference between measured and calculated values
24.17	.8130	.812087	1.31726E-05
20.14	.8283	.824591	3.60942E-03
23.72	.8185	.814282	4.21751E-03
23.93	.8129	.813678	-7.77900E-04
0.90	.8788	.879989	-1.18911E-03
13.07	.8450	.844948	5.24521E-05
20.53	.8223	.823468	-1.16766E-03
22.27	.8167	.818458	-1.75756E-03
24.26	.8128	.812728	7.23600E-05
26.19	.8071	.807171	-7.05719E-05
28.01	.8001	.801930	-1.83016E-03
37.31	.7736	.775152	-1.55222E-03
47.95	.7449	.744516	3.83073E-04

The calibration of the Rapid-k was performed for values of $\dot{H}$ ranging from 0 to 100 $W \cdot m^{-2}$. The upper extremity of the range was limited by the low melting point temperature of the acrylic used to frame the standard specimen. Before each calibration test, the specimen was dried in an oven for 15 hours at 70°C, since the R value given by NRC was for a dry specimen. The values of temperature and voltage were considered to be at thermal stability when the ratio of voltage from the heat flow meter over ΔT varied less than 1% over a period of 20 minutes.

Figure 3 depicts the calibration curve of the Rapid-k, representing the relationship between the calculated $\dot{H}$ in W•m-2 and the voltage output of the heat flow transducer in mV. The highly significant ($p < 0.001$) linear relationship can be described as follows:

$$\dot{H} = 27.5092 \cdot V - 0.0044 \qquad (6)$$

$$r = 0.999$$

By varying the temperature of the heat flow meter of the Rapid-k from 5 to 30°C (i.e., the cold plate temperature), a variation in the voltage output of less than 1% was observed for the same calculated $\dot{H}$ values. It can therefore be concluded that the relationship between the calculated $\dot{H}$ and V is temperature independent at least for this calibration temperature range.

2.2 Characterization of HFTs

Two waterproof versions of HFTs available on the market (one made by Thermonetics Corporation and the other by Concept Engineering) were chosen for evaluation because they offer the best potential for the measurement of heat flow in a variety of environments.

Figures 4 and 5 depict the characteristics of the two types of HFT discs. The HFTs from Thermonetics are 1.1 to 2.1 times more sensitive, but more fragile than those from Concept. We observed that the Thermonetics HFT is susceptible to mechanical breakdown at the junction between the disc and the wire. Because the Concept HFT is provided without the wire (the wire is optional), the strength of the junction depends upon the material used to seal the connection between the HFT and the wire. Another difference between the two HFT discs is the location of the thermistor on the disc. The placement of the thermistor on the edge of the Thermonetics HFT makes it more susceptible to thermal measurement error due to the edge effect described by Wissler and Ketch (14). In both cases however, the thermistor measures the temperature of the skin under the HFT, which can be different from the temperature of the skin not covered by the HFT (14).

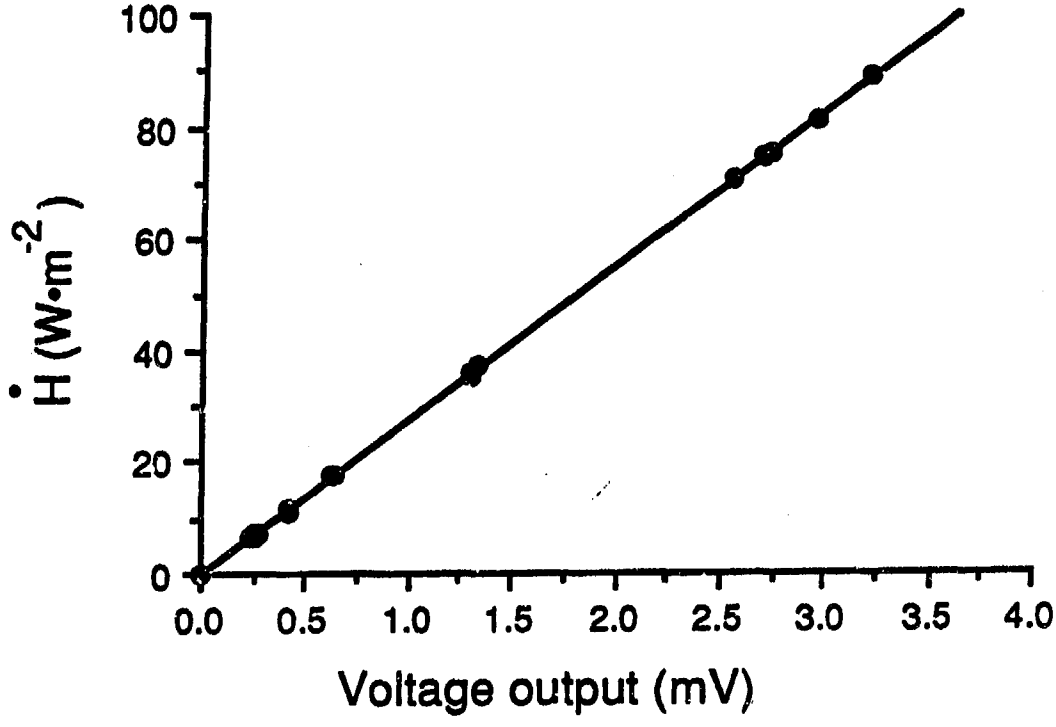

Figure 3: Calibration curve of the Rapid-k instrument representing the voltage output from the heat flux meter of the Rapid-k (mV), and the calculated heat transfer $\dot{H}$ (W•m^{-2}).

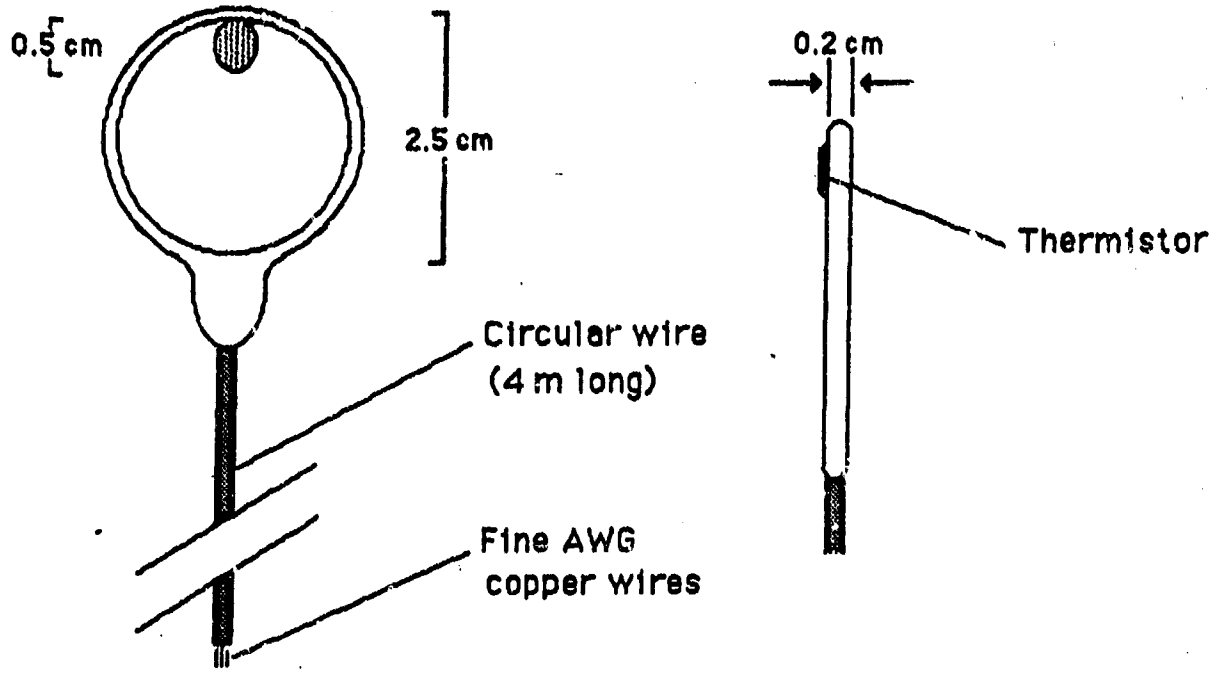

Model #: HA13-18-10-P(C)

Factory calibration constant: 60 to 100 $W \cdot m^{-2} \cdot mV^{-1}$

Sensitivity: 10 to 17 $\mu V \cdot m^2 \cdot W^{-1}$

Accuracy: 10%

Impedance: 162 ohms

Factory stated thermal conductivity: 0.225 $W \cdot m^{-1} \cdot {}^{\circ}C^{-1}$

Thermistor type: YSI 44018 (temperature range: -30 to 105 °C)

price: US $170.00/unit

Time delay to order: several months

Address of manufacturer: Thermonetics Corporation
Box 9112 San Diego,
California 92109
U.S.A.
tel: (619) 488-2242

Figure 4: Characteristics of the heat flux transducer from Thermonetics Corporation.

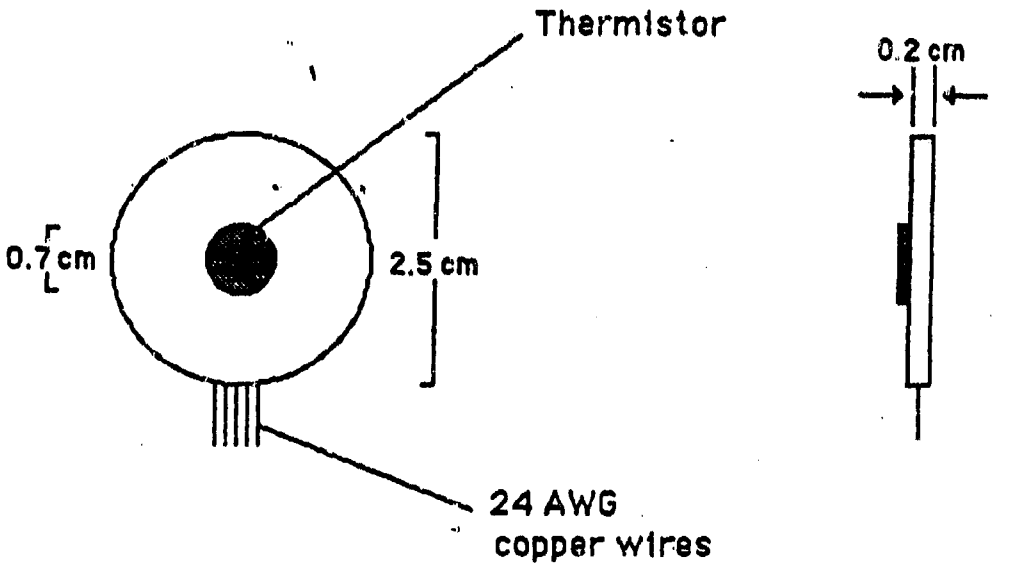

Model #: FR-040-TH44018 (without wire)

Factory calibration constant: 110 to 125 $W \cdot m^{-2} \cdot mV^{-1}$

Sensitivity: 8 to 9 $\mu V \cdot m^2 \cdot W^{-1}$

Time constant: 7 sec

Impedance: 175 ohms, nominal

Factory stated thermal conductivity: 0.4615 $W \cdot m^{-1} \cdot {}^{\circ}C^{-1}$

Thermistor type: YSI 44018 (temperature range: -30 to 105 ° C)

Price: US $190.00/unit

Time delay to order: several weeks

Address of manufacturer: Concept Engineering
43 Ragged Rock Road
Old Saybrook
CT 06475 U.S.A.
tel: (203) 388-5566

Figure 5: Characteristics of the heat flux transducer from Concept Engineering.

2.3 Calibration of HFTs

The method of calibration for the HFTs presented in this section is an adaptation of the method described by Nuckols and Piantadosi (7).

During the calibration tests, the HFTs were held firmly within a test bed in the test section of the Rapid-k. The reasons for using a test bed were: 1) to create a range of heat flow through the HFTs similar to that expected from the body under different environmental conditions (from 0 to 500 $W \cdot m^{-2}$); 2) to optimize the homogeneity of heat flow around the HFTs; and 3) to ensure good surface contact with the HFTs. The criteria for the selection of the test bed materials were: 1) resistance to heat deformation; 2) a value of thermal conductivity close to the k value of the HFTs (between 0.2 and 0.4 $W \cdot °C^{-1} \cdot m^{-1}$); and 3) some practical considerations (availability, cost and ease of machining). Two different materials met those requirements: Teflon, with a k value of 0.24 $W \cdot °C^{-1} \cdot m^{-1}$; and hardboard wood with k = 0.20 $W \cdot °C^{-1} \cdot m^{-1}$ (1). Figure 6 shows the test bed used for the calibration tests. It was comprised of two parts; namely, the test bed matrix and the HFT support. Because of the cost of teflon, only the HFT support was made of this material. Four HFTs were positioned in the HFT support within the central 10 cm x 10 cm effective area where $\dot{H}$ is measured by the heat flow meter of the Rapid-k. They were held in place by a layer of the same type of tape as that used to fix the HFTs over the skin (Blenderm surgical tape, 3M Corporation). To optimize the heat transfer from the test bed to the HFTs, the interfaces were filled with a thermally conductive grease (Thermal compound part no. 120-2, Wakefield Engineering, Wakefield, MA). Figure 7 presents the complete test setup of the system within the effective area of the test section of the Rapid-k as used during a calibration run.

During the calibrations, the transducers were exposed to heat flows ranging from 0 to 500 $W \cdot m^{-2}$ by varying the temperature of the hot plate from 30 to 95°C. The temperature of the cold plate was maintained constant at approximately 30°C to minimize the effect of temperature on HFT responses and to avoid the change in k value of the HFTs with temperature. The HFT, thermocouples and Rapid-k heat flow meter output voltages were read with a computer controlled data acquisition system (HP-85 computer, HP-3495 scanner, HP-3455A digital voltmeter; Hewlett-Packard Corporation). After each minute of scanning, a mean value was calculated for each transducer. The program used for the calibration of the HFTs is presented in Annex A. Only values obtained during steady state were used to calculate the HFT calibration constants. Thermal steady state was considered established when the ratio of measured heat flux from the Rapid-k ($\dot{H}$) to temperature differential ($\Delta T = T_{hot} - T_{cold}$) did not change by more than 1% over a 20-min period. The calculations of the HFT calibration constants were made by transforming the voltage output of the Rapid-k heat flow meter into heat flow $\dot{H}$ using the previously established calibration curve of the Rapid-k, and by using the voltage output of the HFT (mV) under investigation as follows:

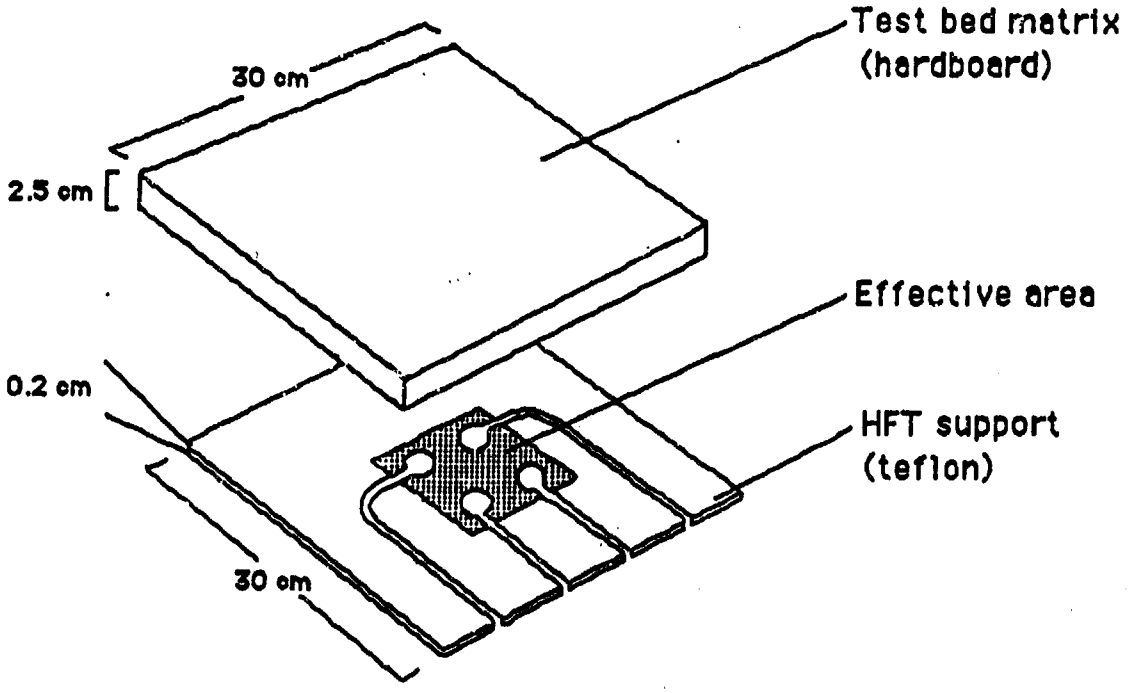

Figure 6: Representation of the test bed used for the calibration of the HFTs. It was comprised of the test bed matrix and the HFT support. Four HFTs were positioned on the HFT support in the effective area.

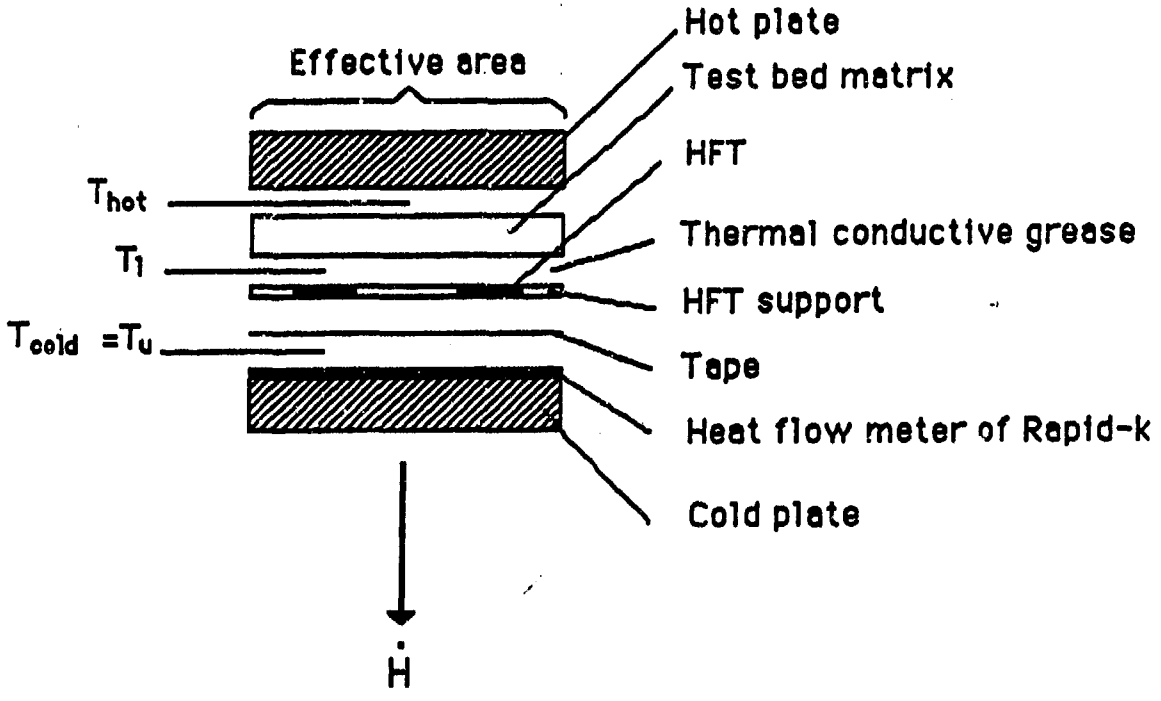

Figure 7: Representation of the effective area of the test section for the calibration and the determination of k value of the HFTs. T_{hot}, T_l and T_u represent the location of the thermocouples used to determined the HFT thermal conductivities.

$$\text{calibration constant} = \frac{\dot{H}_{\text{Rapid-k}}}{V} \qquad (7)$$

where the calibration constant is expressed in $W \cdot m^{-2} \cdot mV^{-1}$.

To define the effects of temperature on HFT response, four transducers were subjected to constant heat flows but to six different temperatures ranging from 10°C to 60°C by varying the cold plate temperature along with the hot plate temperature. In addition, the reproducibility of the calibration method was verified by the recalibration of four HFTs over a two-week period.

Verification of the consistency of our calibration method was obtained using a double layer HFT test. This test consisted of measuring the value of heat flow passing through two superimposed HFTs sandwiched between two pieces of hard board (see Fig. 8). Since the heat flow is the same through the two HFTs, the calculated values of $\dot{H}$, using the calibration constants determined by the Rapid-k and the signal output of each HFT, should be equal if the calibration method is consistent.

2.4 Determination of HFT thermal conductivity

The determination of the thermal conductivity value for the HFTs was performed at the same time as the calibration tests (see Fig. 7). For each HFT in the test bed, two calibrated fine gauge thermocouples (AWG 40) were fixed on the opposite surfaces of the transducer (T_l and T_u). The k values of the HFTs were calculated using the Fourier linear heat flow equation as follows:

$$k = \frac{\dot{H}_{\text{Rapid-k}} \cdot x}{T_l - T_u} \qquad (8)$$

where k is the thermal conductivity of the HFT and the tape in $W \cdot °C^{-1}$ m^{-1} is the thickness of the HFT plus the tape in m, and $T_l - T_u$ is the temperature difference between the two opposite surfaces of the HFT including the tape in °C. The tape is included in the calculation of the k value because, when used over the HFT to fix the transducer on the skin, it acts, like the HFT, as an insulative material. The thermal resistance of the HFT, R_T, is x/k and is in units of $°C \cdot m^2 \cdot W^{-1}$.

2.5 Correction for the thermal resistance of HFTs

2.5.1 Validation of the proposed equations

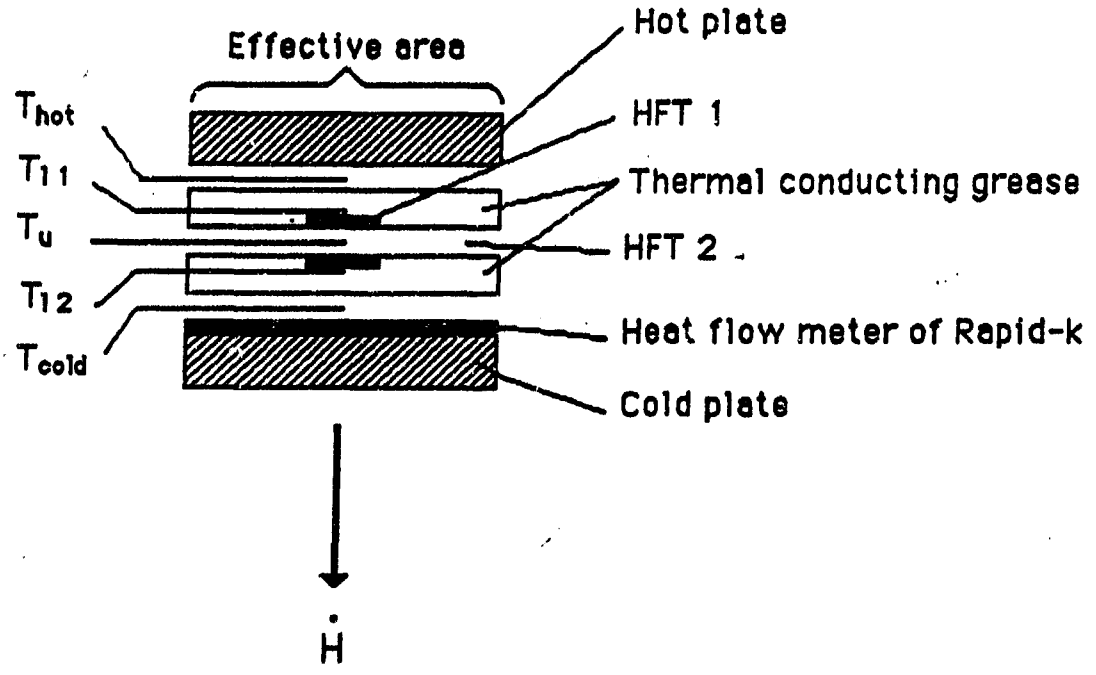

Figure 8: Representation of the effective area of the test section for the double layers HFT tests. The HFT support is made with two 1.3 cm thick layers of hardboard wood.

Three different equations have been proposed in the literature to correct the measured values of thermal flux for the effect of the thermal insulation of the HFTs (6, 13, 14). The proposed equations are the following:

i) Strong et al. (13)

$$\dot{H}_{corr} = \frac{(T_{sk} - T_w) \bullet \dot{H}_{meas}}{(T_l - T_w) - R_T \bullet \dot{H}_{meas}} \tag{9}$$

ii) rearranged from the equation of Gin et al. (6)

$$\dot{H}_{corr} = \frac{(T_c - T_{sk}) \bullet \dot{H}_{meas}}{(T_c - T_l)} = \frac{T_c - T_{sk}}{(T_c - T_u)/\dot{H}_{meas} - R_T} \tag{10}$$

iii) Wissler and Ketch (14)

$$\dot{H}_{corr} = \frac{\dot{H}_{meas}}{1 - \dot{H}_{meas} \bullet R_T/(T_c - T_w)} \tag{11}$$

where $\dot{H}_{corr}$ is the thermal flux through the skin corrected for the insulating effect of the HFT ($W \bullet m^{-2}$), $\dot{H}_{meas}$ is the measured heat flow value ($W \bullet m^{-2}$), T_c is the core temperature of the segment for which the heat flux is measured (°C), T_{sk} is the temperature of the uncovered skin of the segment (°C), T_l is the temperature of the skin under the HFT (°C), T_u is the temperature of the upper surface of the HFT (°C), T_w is the water temperature (°C), and R_T is the thermal resistance of the HFT ($°C \bullet m^2 \bullet W^{-1}$).

Although all the above equations are theoretically equivalent (see Annex B for demonstration), some of them differ in practice due to the difficulties of obtaining accurate values for the parameters. Application of the equations to experimental data has shown that the Strong equation (13) is too sensitive to temperature measurement errors (as low as 0.05°C), which makes it impractical. On the other hand, the equations rearranged from Gin et al.'s study (6) require measurements of the temperatures of the surfaces of the HFTs. These are difficult to measure accurately, and therefore can easily lead to error when $\dot{H}_{corr}$ is calculated. The application of Wissler and Ketch's (14) equation to experimental data has shown it to be useable. The only practical limitation of this equation is the measurement of the parameter T_c, the core temperature of the segment under consideration. If it cannot be measured, one might obtain an estimate from

mathematical modelling.

2.5.2 Effect of the insulation of the underlying body tissue on the relative error in thermal flux

The equation proposed for the correction of the thermal resistance of HFTs (i.e., equation iii) shows that the correction factor ($\dot{H}_{corr}/\dot{H}_{meas}$) in thermal flux is proportional to the thermal resistance of the transducer (R_T), but inversely proportional to the total thermal resistance from core to ambient (T_c-T_a /$\dot{H}_{meas}$), as expected. In addition, Gin et al. (6), and later Wissler and Ketch (14), suggested that the relative error in thermal flux is also dependent upon the underlying insulation of the body tissue. When the HFTs are used under cold stress causing cutaneous vasoconstriction, the error in thermal flux seems unimportant (6), but when used under conditions that do not produce vasoconstriction, the error in thermal flux may approach 15% (14).

However, to our knowledge, no additional information is available in the literature on the effect of the underlying insulation of the body tissue on the relative error in thermal flux due to the thermal resistance of the HFT.

2.5.2.1 The variable-R model

In order to assess the relationship between the underlying tissue insulation and the error in thermal flux due to the thermal resistance of HFT, a model system was developed to create a large range of "tissue" thermal resistance values (see Fig. 9). The variable-R model consisted of an insulated water-filled copper box (maintained at 37°C with a proportional temperature controller) immersed in a water bath maintained at 30°C with a second proportional temperature controller. The thermal insulation of the model was varied by changing the material type (polystyrene, neoprene, hard board wood, aluminum and copper) and thickness (1 mm to 13 mm) on one wall to give insulation values ranging from $2.7\text{x}10^{-4}$ to $4.4\text{x}10^{-1}$ °C•m^2•W^{-1}. For each setting, the thermal flux through the system was measured with 3 calibrated HFTs (either from Thermonetics or Concept Engineering) fixed on the external surface of the insulation with Blenderm surgical tape. The interfaces between the copper wall of the variable-R model and the insulative material, and between the insulative material and the HFT, were filled with thermally conductive grease. The "skin" temperature of the model (T_{sk}) was measured with a fine type T calibrated thermocouple. The thermal insulation of the model (R_m, in °C•m^2•W^{-1}) was calculated as follows:

$$R_m = \frac{T_c - T_{sk}}{\dot{H}_{corr}} \qquad (12)$$

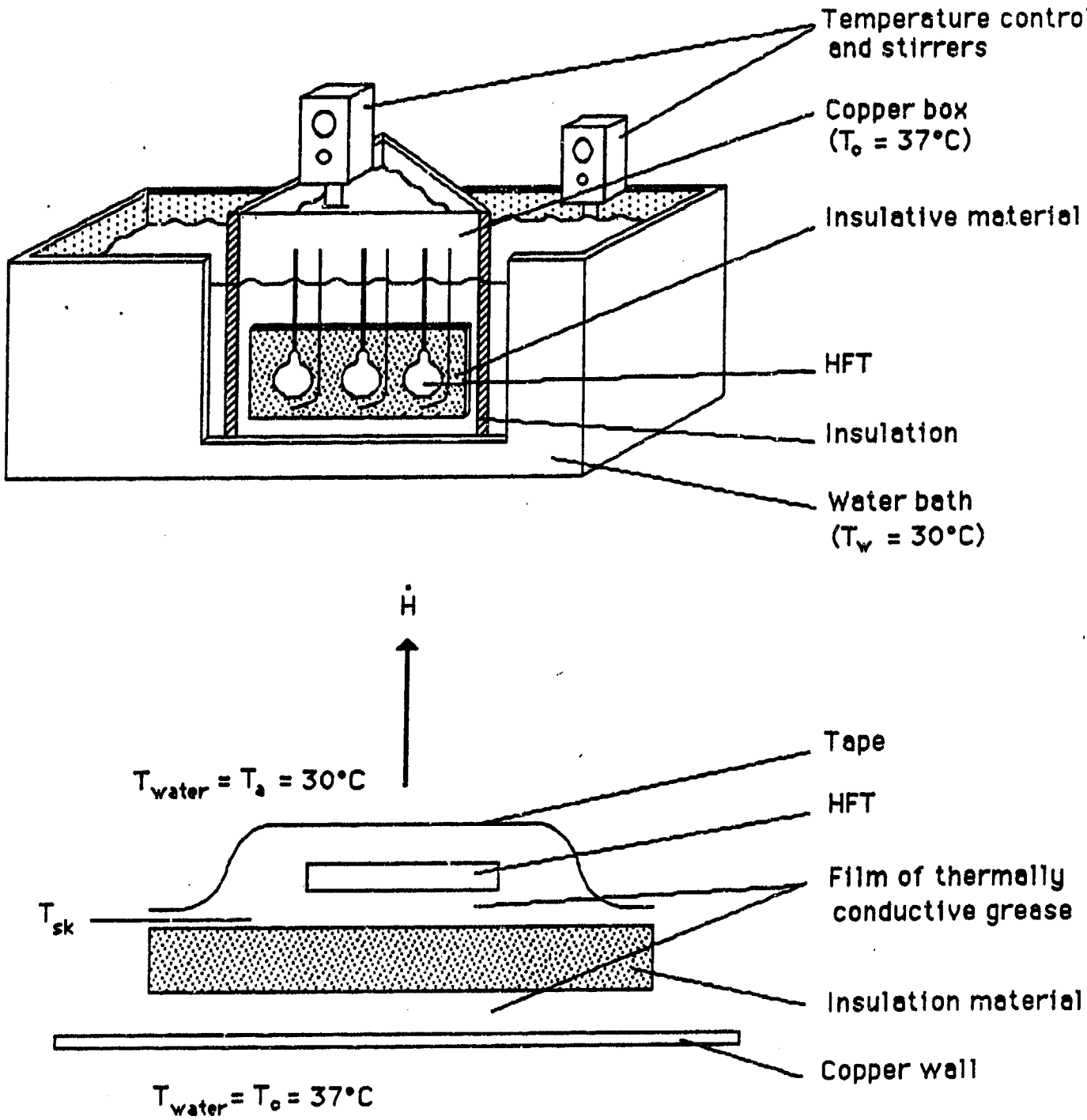

Figure 9: The variable-R model used for the study of the relationship between the underlying tissue insulation and the relative error in thermal flux due to the thermal resistance of HFTs. The thermal resistance of the model wall (copper box) was varied by using different insulative material and thickness.

where T_c was the core temperature of the model (37°C), $\dot{H}_{corr}$ was calculated by using Wissler and Ketch's (14) equation. The thermal insulation values were calculated using the mean values of thermal flux and temperature recorded during the last 10 minutes of each experiment, when thermal stability was achieved.

2.5.2.2 Tests with human forearms immersed in water

The objective of these tests was to validate the data from the variable-R model with experimental data from immersions of human forearms exposed at different water temperatures.

The methods used during the study were approved by DCIEM Human Ethics Committee. The experiments involved ten healthy male subjects between 18 and 30 years of age. Each experiment consisted of immersing the forearm in a water bath for 3 hours at a constant temperature ranging between 15 and 36°C. These water temperatures were chosen in order to create a large range of tissue insulation. Each subject experienced two different temperatures chosen randomly, one for each forearm, over a two-week period. During the experiments, the subjects were in a sitting position, and the ambient temperature of the room was 25 ± 1°C. A total of 20 experiments were performed.

The muscle temperature (T_m) was continuously monitored during the immersions at each 5 mm of tissue from the longitudinal axis of the forearm (determined from computed tomography scanning) to the skin on the proximal third of the limb (superficial muscle: *flexor carpi ulnaris*; deep muscle: *flexor digitorum prolundus*). The temperature of the muscle was recorded with a fine calibrated multicouple probe implanted under local anaesthesia (skin refrigerant, Ethyl Chloride; Graham-Field, N.Y.) by using a method detailed elsewhere (4). The temperature values were corrected for the thermal conductivity effect along the wires of the probe (4). The maximal value of T_m, always found at the longitudinal axis of the forearm, was used to represent T_c, the core temperature of the segment. The other physiological parameters recorded during the immersions were the heat flux through the skin of the forearm with a recalibrated Thermonetics HFT, and the skin temperature with a fine calibrated 40 gauge thermocouple probe. Both the HFT and the thermocouple were fixed a few millimetres beside the site of the muscle temperature measurements using Blenderm surgical tape.

The $\dot{H}_{corr}$ values were calculated by using the Wissler and Ketch correction previously described (14). All thermal flux and temperature values used in the calculations were from the last 15 minutes of each experiment, when thermal stability was achieved.

2.6 Statistical analyses

The different linear and curvilinear regression analyses and independent t-tests presented throughout this study were performed with the BMDP statistical programs (BMDP Statistical Software, 1983, Los Angeles, California). The values are expressed as mean ± S.D.

3. RESULTS

3.1 Calibration of HFTs

All HFTs from Thermonetics and Concept showed linear responses over the calibration heat flux range of 0 to 500 $W \cdot m^{-2}$. The correlation between the HFT voltage output and the Rapid-k heat flow is highly significant ($p < 0.001$) for each HFT calibrated. Each transducer response had a different slope, but the linearity of the responses and the nearly zero intercepts support the use of a constant calibration factor for each transducer over the test range of heat flow. An example of the linearity of the response is presented in Fig. 10 for 4 HFTs from Thermonetics.

The calibration constants determined by the Rapid-k for 15 HFTs from Thermonetics Corp. and 12 HFTs from Concept Engineering, and those constants provided by the manufacturers are presented in Table 2. The mean difference between our calibration constants and the factory constants is 20.2 ± 7.1% (8.3 to 32.2%) for the Thermonetics HFTs and -0.7 ± 4.8% (-8.6 to 8.8%) for the Concept HFTs (4.0 ± 2.5% in absolute value ignoring the signs). The mean difference value is significantly different from 0 for the Thermonetics HFTs ($p < 0.001$), but not for the Concept HFTs ($p > 0.05$). Both mean difference values are significantly different from one another ($p < 0.001$). The repeat calibrations of 4 HFTs over a two-week period gave a mean variability of less than 2% from the first determination, which confirms the reproducibility of our technique. In addition, the calculated heat flow values from two superimposed HFTs, using the respective calibration constants and voltage outputs, gave for three tests a mean difference between the two values of less than 2%. These results confirmed the consistency of the calibration between HFTs. In addition, as shown in Fig. 11, the temperature of the HFT had no significant effect ($p > 0.05$) on the calibration constant for the 4 HFTs tested over a range of temperatures between 10 and 60°C.

3.2 Thermal conductivity of HFTs

The mean value of the thermal conductivity of the HFTs at 30°C determined by the Rapid-k is 0.194 ± 0.018 $W \cdot °C^{-1} \cdot m^{-1}$ ($n = 17$) for the Thermonetics HFTs and 0.316 ± 0.015 $W \cdot °C^{-1} \cdot m^{-1}$ ($n = 15$) for the Concept Engineering HFTs. The two values are significantly different ($p < 0.001$) and specific to the construction characteristics of each type of HFT. The mean difference between the k value determined by the Rapid-k and the factory value is 16.0% for the Thermonetics HFTs, and 46.0% for the Concept HFTs.

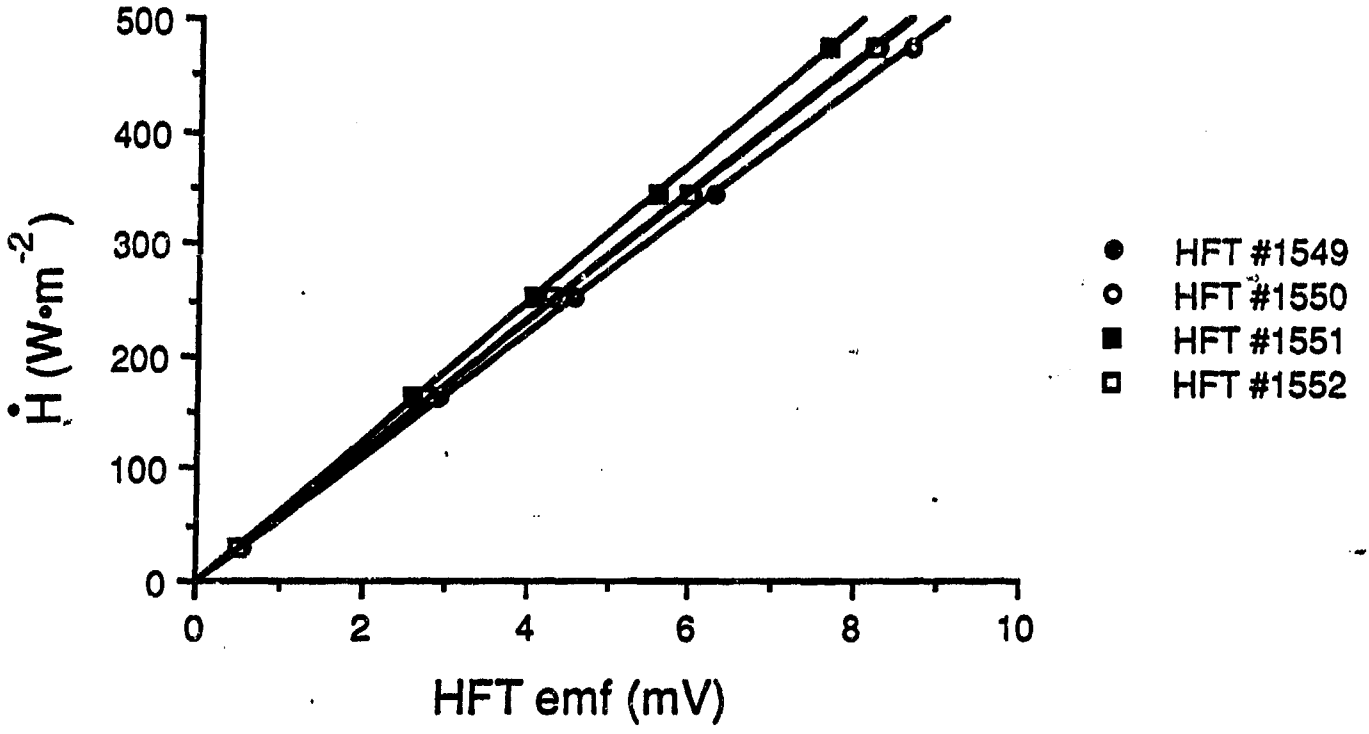

Figure 10: Examples of the linear relationship between the HFT voltage output and the Rapid-k heat flux for 4 HFTs from Thermonetics Corporation.

Table 2: List of the thermal constants for 15 HFTs from Thermonetics Corporation and 12 HFTs from Concept Engineering, determined by the manufacturers and during the recalibration tests.

A. HFTs from Thermonetics Corporation

Serial number	Thermal constant from manufacturer ($W \cdot m^{-2} \cdot mV^{-1}$)	Thermal constant from recalibration ($W \cdot m^{-2} \cdot mV^{-1}$)	Percentage of deviation (%)
1549	64.7	55.316	17.0
1550	69.4	56.357	23.1
1551	71.0	62.460	13.7
1552	69.4	58.556	18.5
1553	71.0	57.912	22.6
1554	69.4	57.358	21.0
1558	69.4	62.427	11.2
1559	72.5	66.925	8.3
1560	72.5	62.902	15.3
1561	80.4	61.535	30.7
1562	94.6	77.515	22.0
1563	71.0	60.962	16.5
1564	74.1	56.458	31.3
1565	93.0	70.332	32.2
1566	72.5	60.900	19.1
			Mean 20.2±7.1

B. HFTs from Concept Engineering

Serial number	Thermal constant from manufacturer ($W \cdot m^{-2} \cdot mV^{-1}$)	Thermal constant from recalibration ($W \cdot m^{-2} \cdot mV^{-1}$)	Percentage of deviation (%)
1118	111.04	116.758	-4.9
1122	123.66	120.205	2.9
1123	123.66	126.817	-2.5
1120	123.66	121.355	1.5
1119	118.29	123.095	-3.9
1115	117.03	128.000	-8.6
1121	120.82	123.246	-2.0
1116	118.29	122.681	-3.6
1172	124.35	127.562	-2.5
1173	119.00	113.254	5.1
1175	114.20	112.355	1.6
1176	114.20	104.293	8.8
			Mean -0.7±4.8

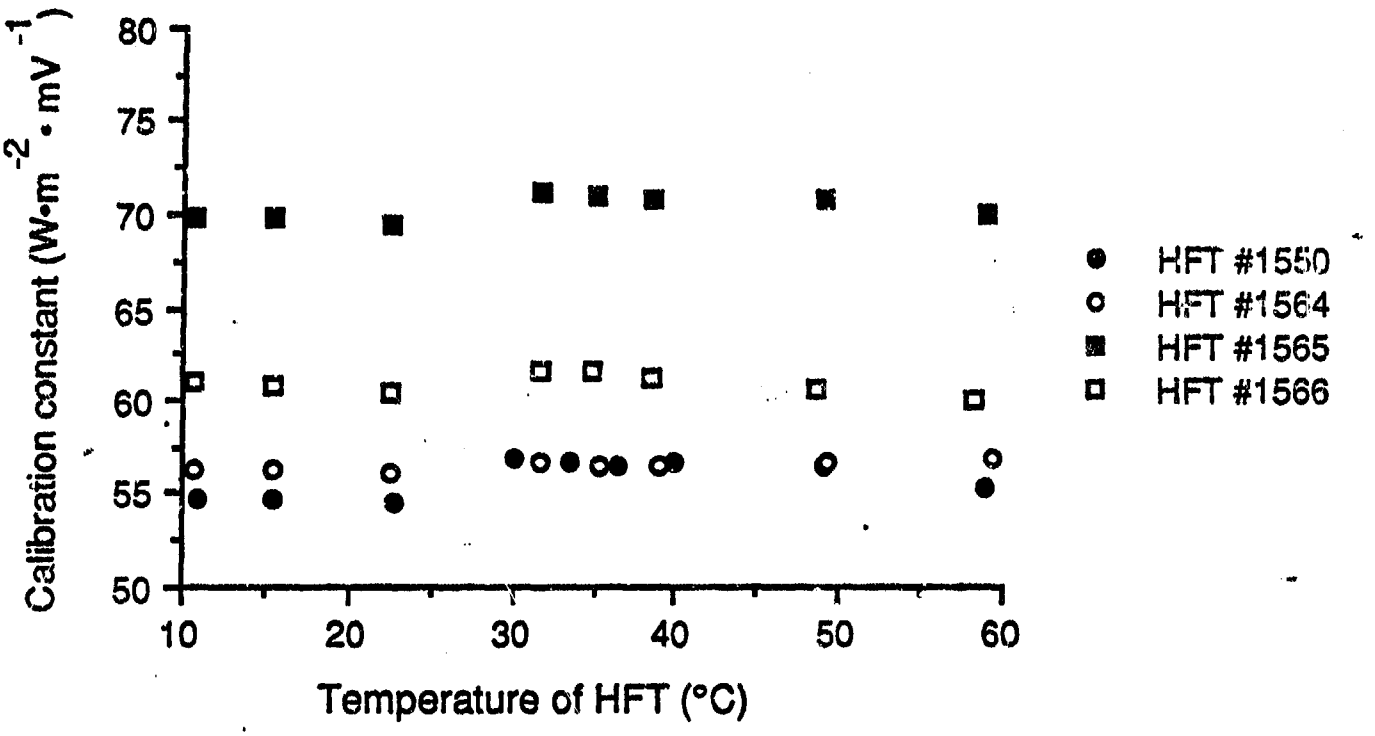

Figure 11: Effect of temperature on the calibration constant determined during the recalibration tests for 4 HFTs from Thermonetics Corporation.

3.3 Relationship between the underlying "tissue" insulation and the relative error in thermal flux due to the thermal resistance of the HFT

3.3.1 The variable-R model

Eight experiments using 3 HFTs from Thermonetics Corp. and 7 experiments using 3 HFTs from Concept were performed using the variable-R model in order to establish the relationship between the underlying "tissue" insulation and the relative error in thermal flux due to the thermal resistance of the HFT. Fig. 12 presents the relationship performed on mean values (3 HFTs for each data point) between the ratio $\dot{H}_{corr}/\dot{H}_{meas}$, which represents the correction factor, and the ratio R_T/R_m for all the range of R_m studied. No significant difference ($p > 0.05$) exists between the relationship determined for each type of HFT. The curvilinear relationship is best described for both types of HFTs by the following equation:

$$\frac{\dot{H}_{corr}}{\dot{H}_{meas}} = 1.721+1.145 \log\frac{R_T}{R_m}+0.688 \left(\log\frac{R_T}{R_m}\right)^2+0.156 \left(\log\frac{R_T}{R_m}\right)^3 \qquad (13)$$

$$r^2 = 0.998$$

When only the physiological range for the ratio R_T/R_m is presented ($R_T/R_m < 0.6$; see ref. 3), the relationship between the ratio $\dot{H}_{corr}/\dot{H}_{meas}$ and the ratio R_T/R_m becomes linear (see Fig. 13). The linear relationship is best described for both types of HFTs by the following equation:

$$\frac{\dot{H}_{corr}}{\dot{H}_{meas}} = 1.004+0.908 \frac{R_T}{R_m} \qquad (14)$$

$$r^2 = 0.999$$

3.3.2 Immersion of the forearm in water

Table 3 presents the temperature and heat flux data for the last 15 minutes of 3 hour immersions of the forearm in water at temperatures ranging between 15 and 36°C ($n = 20$). As expected, the core (T_c) and the skin (T_{sk}) temperatures of the forearm increase with the water temperature (T_w), and the measured values of thermal flux from the skin ($\dot{H}_{meas}$) are inversely

proportional to T_w. The mean values of thermal flux corrected for the thermal resistance of the HFT ($\dot{H}_{corr}$) are 9.8 ± 1.6% higher than $\dot{H}_{meas}$ for $T_w \leq 30°C$, and 25.3 ± 7.0% higher than $\dot{H}_{meas}$ for $T_w > 30°C$.

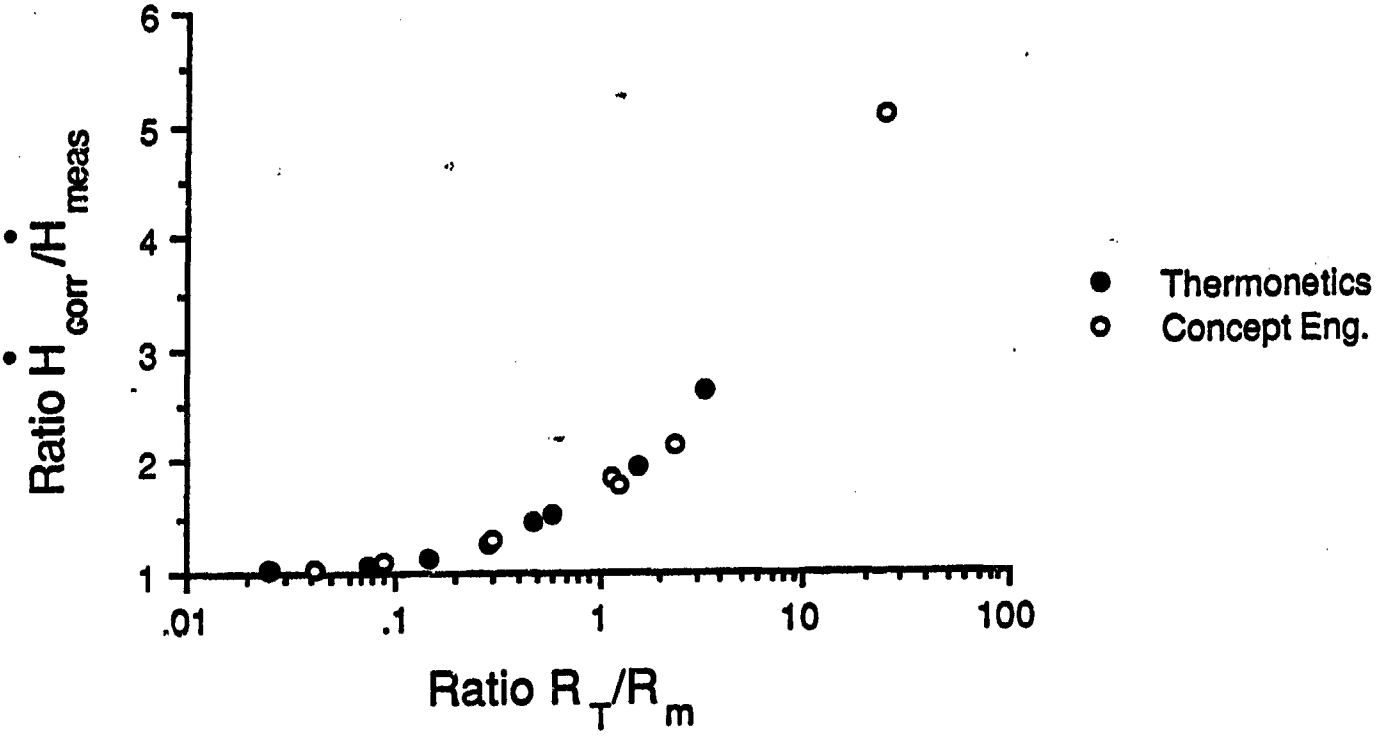

Figure 12: Relationship between the ratio $\dot{H}_{corr}/\dot{H}_{meas}$, which represents the correction factor of the measured thermal flux, and the ratio R_t/R_m, for all the range of R_m studied. The same relationship is valid for both types of HFTs.

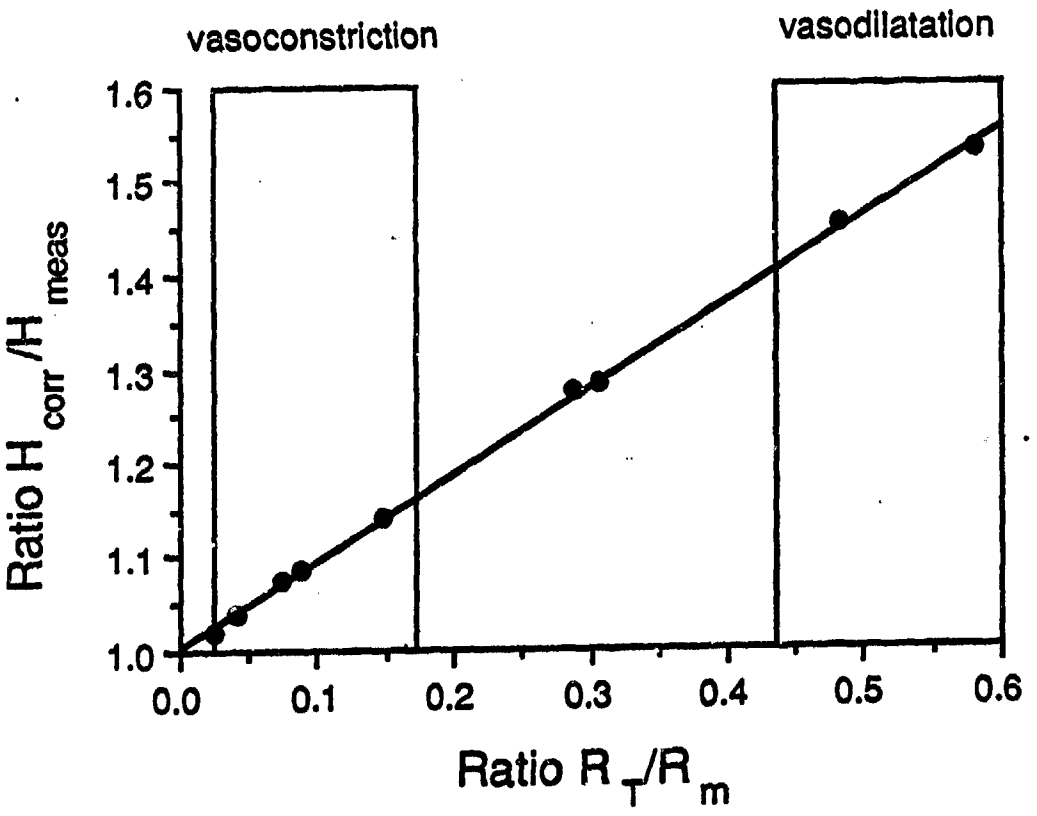

Figure 13: Relationship between the ratio $\dot{H}_{corr}/\dot{H}_{meas}$, which represents the correction factor of the measured thermal flux, and the ratio R_t/R_m, for the physiological range of R_m studied. The same relationship is valid for both types of HFTs.

Table 3: Temperature and heat flux data for the last 15 minutes of a 3 hour immersion of the forearm in water at different temperatures. T_w: water temperature (°C); T_{re}: rectal temperature of the subject (°C); T_c: core temperature of the forearm (°C); T_{sk}: uncovered skin temperature of the forearm measured with a fine gauge thermocouple (°C); $\dot{H}_{meas}$: measured heat flux from the skin of the forearm ($W \cdot m^{-2}$); $\dot{H}_{corr}$: heat flux from the skin of the forearm corrected for the insulating effect of the HFT ($W \cdot m^{-2}$); *% dev*: percentage of deviation between $\dot{H}_{meas}$ and $\dot{H}_{corr}$.

	Water temperatures			
T_w (°C)	15	20	30	36
T_{re} (°C)	37.4±0.3	37.5±0.3	37.5±0.2	37.4±0.3
T_c (°C)	24.5±3.0	27.8±1.8	34.3±0.5	36.8±0.2
T_{sk} (°C)	15.2±0.1	20.2±0.1	30.1±0.1	36.1±0.1
$\dot{H}_{meas}$ ($W \cdot m^{-2}$)	83.1±7.2	67.7±10.2	43.2±7.4	22.9±7.1
$\dot{H}_{corr}$ ($W \cdot m^{-2}$)	90.5±7.7	74.0±10.6	48.6±8.6	31.7±12.1
%dev	8.2±0.7	8.5±2.9	10.9±0.8	25.3±7.0

4. DISCUSSION

Because of their convenience, HFTs are being used increasingly to study human thermal physiology under different environmental conditions. However, the vast majority of studies have used the factory calibration data provided with the HFTs, and little attention has been given to the effect of the thermal resistance of the device on the true thermal flux from the skin. The results of this study indicate that the selection and the use of HFTs must be done with care.

4.1 Calibration of HFTs

The recalibrations of HFTs from two companies have shown different deviation values between the factory supplied and the experimentally determined calibration constants. The results indicate that the mean difference (in absolute value) between the experimental calibration constants and the factory constants is 5 times larger in the case of Thermonetics HFTs (20.2%) than for Concept HFTs (4.0%). For each Thermonetics HFT calibrated, the factory constant was overestimated, as opposed to the Concept HFT for which the factory constants were about equally over and underestimated.

These results are consistent with the findings of Nuckols and Piantadosi (7) and of Snellen and Frim (11) who found that the factory calibration constants for the Thermonetics HFTs were on average 9.0% (3 to 20%) and 26.1% (8 to 40%) overestimated, respectively, when compared to the experimentally determined calibration constants. Sowood (12) found that the factory calibration constants for the Concept HFTs differed from his calibration by only 6.2%. The advantage of the present study over the others is that the calibrations of both types of HFTs were performed by the same reliable and reproducible method of calibration over a larger range of thermal flux (from 0 to 500 $W \cdot m^{-2}$), making the comparison between the two types of HFTs more accurate.

The differences between the manufacturer's and the experimental values may be due to an underestimation of the heat flux by the manufacturer's method because the transducers were calibrated prior to waterproofing (9,12), or because the method did not allow for the insulative properties of the disc material (12). Whatever the cause of that difference, it is suggested that in the case of HFTs from Concept Engineering, the devices can be used without recalibration, since the difference between the manufacturer and the experimental calibration data is small (~5%). However, potentially large errors in calculated heat flow may be present when HFTs from Thermonetics are not recalibrated, particularly when transducers with high-percentage calibration errors are placed at heavily weighted skin sites. For this reason, it is recommended to recalibrate individually the Thermonetics transducers before using them. If accurate values of heat flux are required, it is advisable to carefully recalibrate any type of HFTs.

4.2 Correction for the thermal resistance of the transducers

The study involving the variable-R model indicates clearly that a strong relationship exists between the underlying "tissue" thermal resistance and the relative error in thermal flux due to the thermal resistance of the HFT. For high values of "tissue" insulation ($R_t > 0.5°C \cdot m^2 \cdot W^{-1}$; $R_T/R_m < 0.02$; see Fig. 12), the measured value of heat flux is the true thermal flux from the tissue (~0% error), but for very low values of "tissue" insulation ($R_T < 2x10^{-4}°C \cdot m^2 \cdot W^{-1}$; $R_T/R_m > 50$; see Fig.12), an error as high as 500% can be present in the measurement of the thermal flux by an HFT.

To understand this effect, take the example of two systems involving, respectively, a "nearly perfect conductor" (i.e. $R_m << R_T$) and a "nearly perfect insulator" (i.e. $R_m >> R_T$; see Fig. 14). If an HFT is fixed on the conductor, then the HFT becomes the major resistance to the heat transfer through the system at that location. Consequently, heat flow measured at the HFT site ($\dot{H}_{meas}$) will be much less than through the conductor only, and a correction is necessary.

On the other hand, when a "nearly perfect insulator" is used, the insulation R_T added by the HFT to the system ($R_m + R_T$) is negligible as compared to the insulation value of the insulator only. Therefore, the heat transfer through the system is virtually the same as through the insulator only. In that case, the HFT will closely measure the true value of heat transfer through the insulator. It is therefore evident that the difference between $\dot{H}_{meas}$ and $\dot{H}_{corr}$ is highly dependent upon the insulation of the material (or tissue) under the HFT. The deviation from the true value of thermal flux increases with decreasing insulation of the underlying material.

The above interaction becomes particularly important when HFTs are used on highly conductive materials such as metallic skinned mannequins (copper or aluminum). In that case, because the underlying material insulation value is low ($R_T/R_m > 1.5$), the values of heat flux read by the HFTs may underestimate the true value of heat flux by more than 100%, depending on the insulation of the mannequin skin (see Fig. 12). From a physiological standpoint, the underestimation of heat flux through the skin measured by an HFT can be important when the device is used during vasodilatation in warm subjects, as suggested by Gin et al. (6) and Wissler and Ketch (14). For that situation, as shown in Fig. 13, the underestimation of the measured heat flux can range between 29 and 35% from the true value of heat flux (ratio R_T/R_t ranging between 0.45 and 0.6; ref. 3), depending on the HFT model used and the degree of vasodilatation in the tissue. However, when HFTs are used on vasoconstricted skin in cool subjects (ratio R_T/R_t ranging between 0.025 and 0.15; ref. 3), the underestimation of the measured heat flux is much less, ranging between 3 and 13%. It may therefore not be as important to correct the heat flux values for the thermal resistance of the HFT when the device is used on vasoconstricted skin. However, it becomes important to use Wissler and Ketch's (14) equation to correct the measured

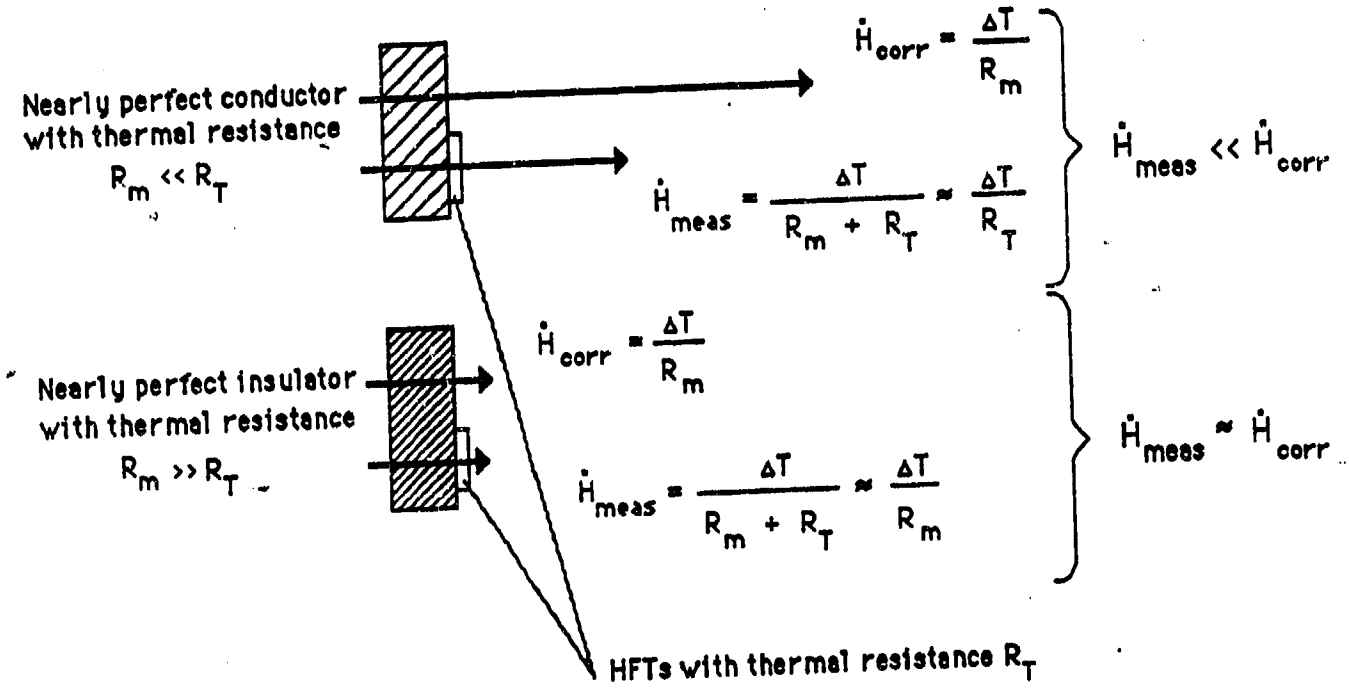

Figure 14: The two thermal systems used to explain the effect of the underlying "tissue" insulation on the correction factor of $\dot{H}_{meas}$ (see text for details).

heat flux for the thermal resistance of the HFT, when the device is used on vasodilated skin. When the correction equations are used, the parameter R_T in the equations (thermal insulation of HFT) has the value of 0.0104°C•m^2•W^{-1} for the Thermonetics HFTs, and 0.0064°C•m^2•W^{-1} for the Concept Engineering HFTs.

Fig. 15 presents a practical example of the magnitude of the error due to the thermal resistance of an HFT when a recalibrated HFT is used to measure the thermal flux from a human forearm immersed in water at different water temperatures. The heat loss from the forearm increases with the reciprocal of water temperature. At water temperatures below the lower critical temperature in water (~30°C; see ref. 10), the tissues are vasoconstricted after immersion in water (2). The % error due to the thermal resistance of the HFT is only 9.8% when the tissues are vasoconstricted, but increases to 25.3% at a water temperature of 36°C where the tissues are partially vasodilated. These data are in agreement with the results found with the variable-R model. They also support the conclusion that the value of thermal flux measured by an HFT should be corrected for the error due to the thermal resistance of the device when the underlying tissues are in a vasodilated state.

4.3 Selection and use of HFTs

Each of the two different models of waterproof HFTs studied presents its own advantages. The HFTs from Thermonetics are more sensitive than those from Concept Engineering. This difference might be noticeable when low values of heat flow are involved, and particularly if the voltage outputs from the HFTs are measured by a voltmeter with low sensitivity. On the other hand, the HFTs from Concept Engineering don't need recalibration, the correction for the thermal resistance of the HFTs is less important (since the thermal conductivity is almost twice that of the Thermonetics HFTs), the temperature reading from the embedded thermistor is less affected by the edge effect (see ref. 14 for details), the disc is less susceptible to mechanical breakdown. But whatever the selection, when properly used and calibrated, both HFTs are equivalent.

To minimize the stress applied on an HFT and to maximize the thermal transfer between the skin and the HFT, the device should be fixed properly on the skin. It is suggested to fix the HFT on the skin with thin surgical tape with the wire parallel to the body segment in the proximal direction. It is recommended to clean, dry and wipe the skin with a protective dressing (Skin Prep, United Medical, FL) prior to attaching the HFT. It is important that the complete surface of the HFT disc makes good contact with the skin. An "S" is made with the wire and then taped to the skin to minimize the stress on the wire (see Fig. 16). During removal, the tape is pulled from the side of the HFT (to reduce the stress at the junction between the wire and the HFT disc) in the same direction as the orientation of the hairs on the skin. To avoid an air or water gap between the HFT and the skin, and to maximize the thermal transfer, it is advised to apply a thin layer of

thermally conductive grease to the surface of the HFT which will be in contact with the skin.

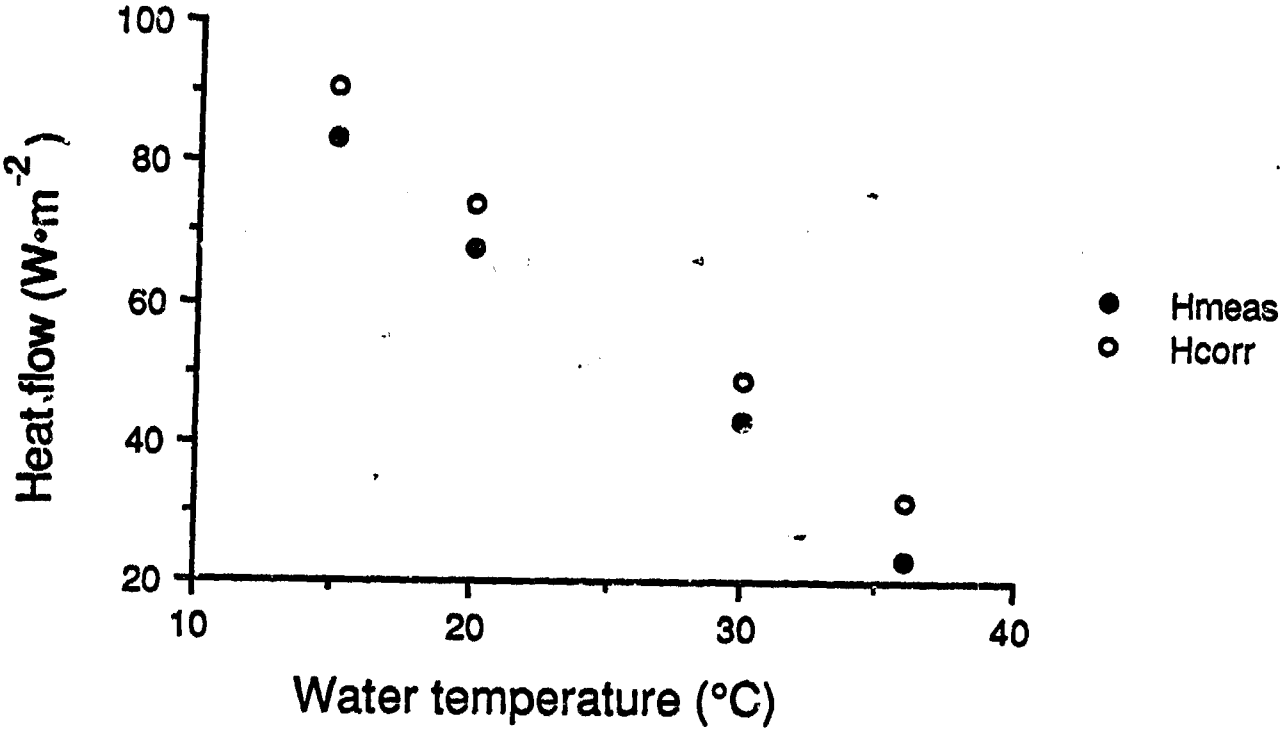

Figure 15: Error involved in the measurement of heat flux from human forearms immersed in water at different temperatures, due to the thermal resistance of HFTs. Each dot represents 5 different subjects. $\dot{H}_{corr}$ was calculated by using Wissler and Ketch's equation (13).

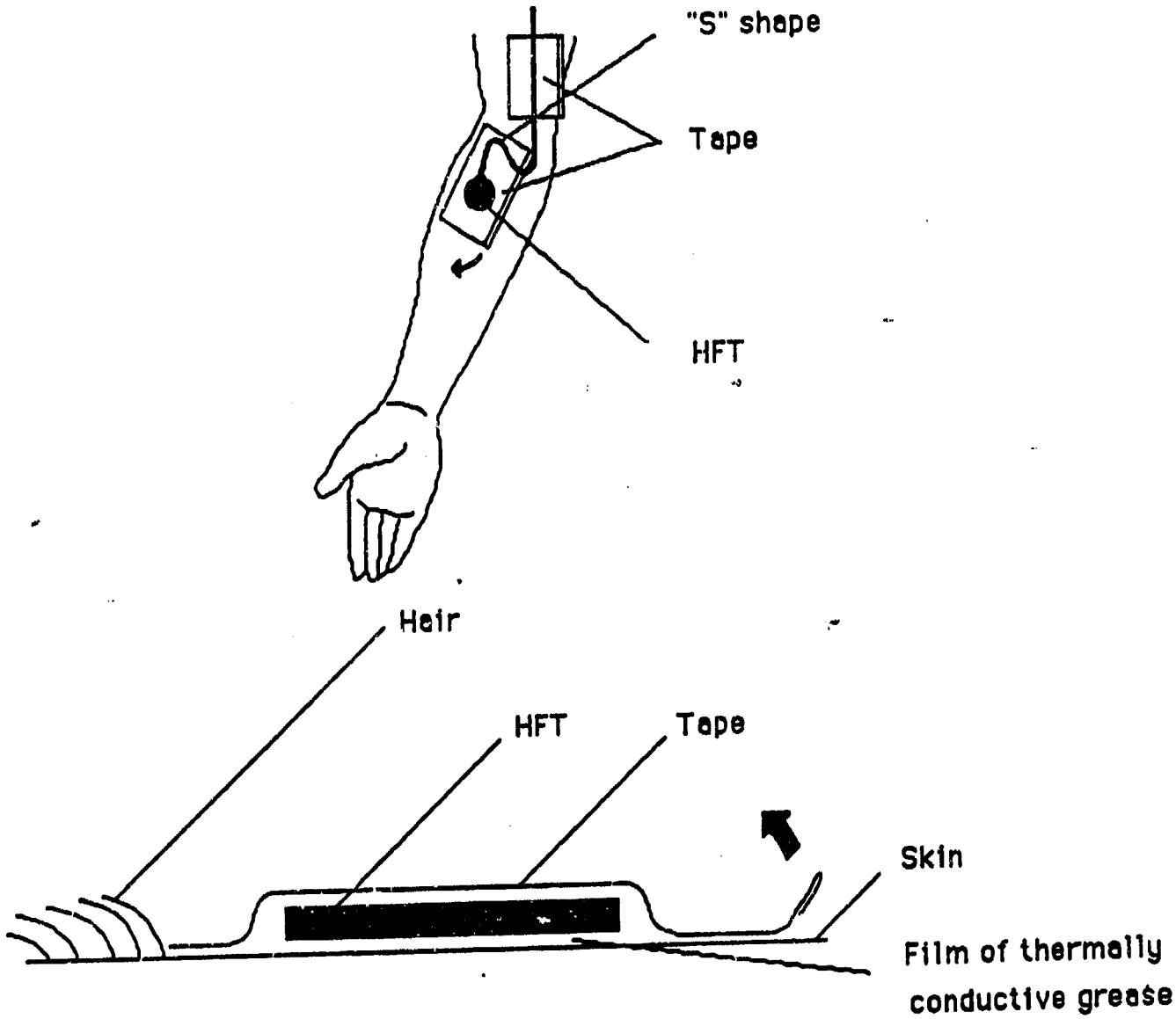

Figure 16: Schematic representation of the suggested method to fix a HFT on the skin to minimize the stress on the HFT and optimize the heat flux from the skin to the HFT.

5. CONCLUSION

The calibrations of two different models of waterproof HFTs have shown significant differences between the recalibration and the manufacturers' constants. Furthermore, a significant difference exists in the error of calibration between the two manufacturers, the error of calibration (in absolute value) being 5 times larger in the case of Thermonetics HFTs. Therefore, it is necessary to recalibrate the Thermonetics HFTs but not those from Concept Engineering. This becomes an important criteria for the selection of HFTs for someone who does not have access to calibration facilities. However, when properly calibrated, both models of HFTs are equivalent. The method presented in this study to calibrate the HFTs using the Rapid-k instrument is easy to use, reliable and reproducible.

The HFTs inevitably underestimate the thermal flux being measured because of the effect of the thermal resistance of the device. By using a variable-R model, it was shown that the magnitude of the underestimation is proportional to the reciprocal of the underlying tissue insulation. The conditions that minimize the deviation from the true value of thermal flux are a low perfusion rate in underlying tissue (vasoconstriction) and a large thermal resistance between the HFT and the environment. The ideal condition for using HFTs is during the measurement of the thermal flux from a dressed subject during exposure to cold air. For that situation, it is less important to apply a correction for the thermal resistance of the transducers. However, the use of HFTs on nude subjects in highly conductive environments (such as water, or high pressure air/or helium-oxygen atmospheres), and particularly under conditions that do not produce vasoconstriction, may cause an underestimation of the thermal flux by the transducer of 30 to 35%. For those particular cases, it is important to correct the measured values of thermal flux for the thermal resistance of the device by using Wissler and Ketch's (14) equation of correction. The heat flux data from experimental immersions of the forearm in water at different temperatures confirmed the results from the variable-R model: the underestimation of the measured heat flux is ~10% during vasoconstriction and approximately ~30% during partial vasodilation of the tissues.

The HFT is a device which represents a compromise between sensitivity and accuracy of measurement. If used properly, it provides useful information within an acceptable range of accuracy. The error in the measurement of the thermal flux should not exceed ~5% when care is taken with respect to calibration and the effect of the thermal resistance of the transducer.

6. ACKNOWLEDGMENTS

The authors gratefully acknowledge Dr. Peter Tikuisis for his contribution to the mathematical demonstration of the equivalence of the different equations proposed to correct for the thermal resistance of HFTs.

7. REFERENCES

1. Bolz, R.E. and G.L. Tuve. CRC handbook of tables for applied engineering science. 2nd edition, CRC Press, Florida, 1166p., 1980.

2. Burton, A.C., H.C. Bazett. A study of the average temperature of the tissue, and of the exchanges of heat and vasomotor responses in man by means of a bath calorimeter. Am. J. Physiol. 117: 36-54, 1936.

3. Cannon, P., and W.R. Keatinge. The metabolic rate and heat loss of fat and thin men in heat balance in cold and warm water. J. Physiol. London 154: 329-344, 1980.

4. Ducharme, M.B., and J. Frim. A multicouple probe for gradient temperature measurements in biological materials. J. Appl. Physiol. 65(5): 2337-2342, 1988.

5. Ducharme, M.B., J. Frim, and P. Tikuisis. Errors in heat flux measurements due to the thermal resistance of heat flux disks. J. Appl. Physiol. 69(2): 776-784, 1990.

6. Gin, A.R., M.G. Hayward and W.R. Keatinge. Method for measuring regional heat losses in man. J. Appl. Physiol. 49(3): 533-535, 1980.

7. Nuckols, M.L. and C.A. Piantadosi. Calibration and characterization of heat flow transducers for use in hyperbaric helium. Undersea Biomed. Res. 7(4): 249-256, 1980.

8. Poppendick, H.F. Why not measure heat flow directly. Environ Q. 15: 1-2, 1969.

9. Poppendick, H.F. A review of calibration methods for small heat flux transducers. Thermonetics Corporation, California, 1979.

10. Rennie, D.W., B.G. Covino, B.J. Howell, S.H. Song, B.S. Kang, S.K. Hong. Physical insulation of Korean diving women. J. Appl. Physiol. 17: 961-966, 1962.

11. Snellen, J.W. and J. Frim. Study of whole body heat exchange with the environment. DCIEM report, DSS File No. 02SE.97711-4-7942, 1987.

12. Sowood, P.J. Calibration of heat flux transducers. Royal Air Force Institute of Aviation Medicine, Scientific memorandum, no. 137, 1986.

13. Strong, L.H., G.K. Gee and R.F. Goldman. Metabolic and vasomotor insulative responses occurring on immersion in cold water. J. Appl. Physiol. 58(3): 964-977, 1985.

14. Wissler, E.H. and R.B. Ketch. Errors involved in using thermal flux transducers under various conditions. Undersea Biomed. Res. 9(3): 213-231, 1982.

ANNEX A
Program used for calibration of HFTs

The program was written in HP Basic Language for a HP-85 computer. The commands used in the program are for the following peripherals: a HP-82901M flexible disc drive, a HP-3495A scanner, a HP-3455A digital voltmeter, a 59309A HP-1B digital clock, a HP-2934A printer and a HP-9872A plotter.

```
10 ! PROG NAME HFTCAL
20 ! PGM HFT CALIBRATION
30 ! BY M DUCHARME
40 !.THIS PROGRAM PRINTS. PLOTS
TEMP & HEAT FLOW DATA FROM RAPID
-K AND HFT
50 ! DATA INCLUDES 10 TEMPS & 2
HFTS
60 ! PROGRAM SCANS CONTINUALLY A
ND SUMS DATA
70 ! 1 MIN SUMS ARE AVERAGED OVE
R N SCANS AND PRINTED
80 ! CH0=Th: CH1=Tc: CH2=Qrapid-
k
90 ! CH6:emfHFT1:CH7:emfHFT2:CH8
:emfHFT3
100 ! CH9:emfHFT4:CH20:TupHFT1:C
H22:TdownHFT1:CH21:Th
110 ! CH23:TupHFT2:CH24:TdownHFT
2
120 ! CH26:TupHFT3:CH27:TdownHFT
3
130 ! CH29:TupHFT4:CH30:TdownHFT
4
140 ! X1:MINIMUM TIME VALUE
150 ! X2:MAXIMUM TIME VALUE
160 ! Y1:MINIMUM VOLT VALUE
170 ! Y2:MAXIMUM VOLT VALUE
180 ! Z1:MINIMUM TEMP VALUE
190 ! Z2:MAXIMUM TEMP VALUE
200 ! N:NUMBER OF SCAN/MIN
210 ! R:NUMBER OF MIN
220 ! T:MONTH VALUE ON CLOCK
230 ! D:DAY VALUE ON CLOCK
240 ! H1:HOUR VALUE ON CLOCK
250 ! M:MINUTE VALUE ON CLOCK
260 ! S1:SECONDE VALUE ON CLOCK
270 ! J:TIME IN SEC
280 ! S:MEAN Th FOR 1 MIN
290 ! U:MEAN Tc FOR 1 MIN
300 ! W:MEAN Q FOR 1 MIN
310 ! V:VOLT FOR TEMP
320 ! T(C):TEMP FOR CHANNEL C
330 ! V1:VOLT FOR Q
340 ! X3:PREVIOUS TIME
350 ! X4:ACTUAL TIME
360 ! F:RATIO W/(S-U)
370 ! N$:NAME OF TEST
380 ! Q1:SCANNER CHANNEL ARRAY
390 ! Q2:SCANNER CHANNEL ARRAY
400 ! L:COUNTER FOR TEMP LOOP
410 ! B:COUNTER FOR VOLT LOOP
420 ! A:MEAN VOLT FROM HFT1
430 ! E:MEAN VOLT FROM HFT2
440 ! G:MEAN VOLT FROM HFT3
450 ! I:MEAN VOLT FROM HFT4
460 CLEAR
470 LINPUT "FILENAME",N$
480 PRINTER IS 701
490 PRINT "FILE:";N$
500 PRINT
510 PRINT
520 PRINT USING 740 : "TIME","ME
AN Th"
530 PRINT USING 740 : "MEAN Tc",
"MEAN Q"
540 PRINT USING 750 : "Q/Th-Tc"
550 PRINT USING 740 ; "","HFT1",
""
560 PRINT USING 740 ; "","HFT2",
""
570 PRINT USING 740 ; "","HFT3",
""
580 PRINT USING 740 ; "","HFT4",
""
590 PRINT
600 PRINT USING 740 : "","","","
"
610 PRINT USING 750 : ""
620 PRINT USING 740 ; "Tup","Tdo
wn","emf"
```

```
630 PRINT USING 740 : "Tup","Tdo
wn","emf"
640 PRINT USING 740 : "Tup","Tdo
wn","emf"
650 PRINT USING 740 ; "Tup","Tdo
wn","emf"
660 PRINT
670 PRINT USING 740 : "(min)","(
deg C)"
680 PRINT USING 740 : "(deg C)",
"(W/m2)"
690 PRINT USING 750 : "(W/m2 deg
 C)"
700 PRINT USING 740 : "(deg C)",
"(deg C)","(mV)"
710 PRINT USING 740 : "(deg C)",
"(deg C)","(mV)"
720 PRINT USING 740 ; "(deg C)",
"(deg C)","(mV)"
730 PRINT USING 740 : "(deg C)",
"(deg C)","(mV)"
740 IMAGE 8,17(12A)
750 IMAGE 8,2(17A)
760 PRINT
770 PRINT
780 PLOTTER IS 705
790 LOCATE
800 X1=0 ! MINIMUM TIME VALUE
810 X2=300 ! MAXIMUM TIME VALUE
820 Y1=0 ! MINIMUM Q VALUE
830 Y2=450 ! MAXIMUM Q VALUE
840 Z1=10 ! MINIMUM TEMP VALUE
850 Z2=100 ! MAXIMUM TEMP VALUE
860 ! *** X AXIS LABEL (TIME)
870 PEN 1
880 SCALE X1,X2,Y1,Y2
890 AXES 10,10,X1,Y1,6,5
900 LORG 6
910 CSIZE 4
920 FOR X=X1 TO X2 STEP 20
930 MOVE X,Y1-(Y2-Y1)*.01
940 LABEL X
950 NEXT X
960 ! *** Y AXIS LABEL (Q)
970 LORG 8
980 FOR Y=Y1 TO Y2 STEP 50
990 MOVE X1,Y
1000 LABEL Y
1010 NEXT Y
1020 LORG 4
1030 MOVE X1+(X2-X1)/2.Y2+(Y2-Y1
)*.01
1040 LABEL N$
1050 ! *** Y AXIS LABEL (TEMP)
1060 PEN 2
1070 SCALE X1.X2.Z1.Z2
1080 AXES X2,1,X2,Z1,1.5
1090 LORG 2
1100 FOR Y=Z1 TO Z2 STEP 5
1110 MOVE X2.Y
1120 LABEL Y
1130 NEXT Y
1140 PEN 1
1150 DEG
1160 LDIR 90
1170 LORG 5
1180 MOVE X1-(X2-X1)*.07,Z1+(Z2-
Z1)/2
1190 LABEL "Q (W/m2)"
1200 LDIR 0
1210 LORG 4
1220 MOVE X1+(X2-X1)/2.Z1-(Z2-Z1
)*.1
1230 LABEL "TIME (min)"
1240 PEN 2
1250 LDIR 90
1260 LORG 5
1270 MOVE X2+(X2-X1)*.07.Z1+(Z2-
Z1)/2
1280 LABEL "TEMPERATURE (deg C)"

1290 PEN 0
1300 CLEAR
1310 DISP "PRESS 'CONTINUE' TO S
TART"
1320 PAUSE
1330 !
1340 !
1350 R=0
1360 N=0
1370 OUTPUT 722 :"F1R7T3M0H1"
1380 CLEAR
1390 OUTPUT 708 ;"PR"
1400 OUTPUT 708 ;"T"
1410 R=R+1
1420 GOSUB 1560 ! SCANSTART
1430 GOSUB 1660 ! SCAN
1440 ENTER 708 ; T,D,H1,M,S1
1450 J=S1+60*M+3600*H1
1460 IF J/60<R THEN 1430
1470 GOSUB 1970 ! CALSCAN
1480 GOSUB 2060 ! PRINT
1490 IF R>1 AND R MOD 5=0 THEN G
OSUB 2190 ! PLOT
```

```
1500 GOSUB 2540 ! UPDATE
1510 GOTO 1410
1520 STOP
1530 !
1540 !
1550 ! SCANSTART
1560 S=0
1570 U=0
1580 W=0
1590 N=0
1600 A=0
1610 E=0
1620 G=0
1630 I=0
1640 RETURN
1650 ! SCAN
1660 N=N+1
1670 ! TEMP_SCAN
1680 DIM Q1(8)
1690 DATA 21,20,22,23,24,26,27.2
9,30
1700 MAT READ Q1
1710 FOR L=0 TO 8
1720 OUTPUT 709 USING "DDD" ; Q1
(L)
1730 OUTPUT 722 :"VT3"
1740 ENTER 722 ; V
1750 T(L)=(V*1000)^2*(-.671)+25.
897*1000*V-.01
1760 NEXT L
1770 S=S+T(0)
1780 U=U+(T(1)+T(3)+T(5)+T(7))/4

1790 ! VOLT_SCAN
1800 DIM Q2(4)
1810 DATA 2,6,7,8,9
1820 MAT READ Q2
1830 FOR B=0 TO 4
1840 OUTPUT 709 USING "DDD" ; Q2
(B)
1850 OUTPUT 722 ;"VT3"
1860 ENTER 722 ; V1
1870 V(B)=V1*1000
1880 NEXT B
1890 W=W+V(0)
1900 A=A+V(1)
1910 E=E+V(2)
1920 G=G+V(3)
1930 I=I+V(4)
1940 RESTORE
1950 RETURN
1960 ! CALSCAN
1970 S=S/N
1980 U=U/N
1990 W=-.0044+27.5092*(W/N)
2000 A=A/N
2010 E=E/N
2020 G=G/N
2030 I=I/N
2040 RETURN
2050 ! PRINT
2060 PRINTER IS 701
2070 F=W/(S-U)
2080 PRINT USING 2130 : R,S,U,W,
F
2090 PRINT USING 2140 : T(1),T(2
),A
2100 PRINT USING 2140 : T(3),T(4
),E
2110 PRINT USING 2140 : T(5),T(6
),G
2120 PRINT USING 2140 : T(7),T(8
),I
2130 IMAGE #,3D,D,7X,3(3D,3D,5X)
,3D,3D,10X
2140 IMAGE #,3(3D,3D,5X)
2150 PRINT
2160 RETURN
2170 PRINT
2180 ! PLOT
2190 X3=R-5
2200 X4=R
2210 SCALE X1,X2,Y1,Y2
2220 MOVE X4,Y1
2230 !
2240 PEN 4
2250 MOVE X3,W0
2260 DRAW X4,W
2270 PENUP
2280 IF X4 MOD 30>5 OR X4 MOD 30
<5 THEN 2330
2290 LDIR 0
2300 LORG 5
2310 MOVE X4,W
2320 LABEL "O"
2330 !
2340 SCALE X1,X2,Z1,Z2
2350 PEN 2
2360 MOVE X3,S0
2370 DRAW X4,S
2380 PENUP
2390 IF X4 MOD 30<15 OR X4 MOD 3
0>15 THEN 2420
2400 MOVE X4,S
```

```
2410 LABEL "Th"
2420 !
2430 PEN 3
2440 MOVE X3.U0
2450 DRAW X4,U
2460 PENUP
2470 IF X4 MOD 30<25 OR X4 MOD 3
0>25 THEN 2500
2480 MOVE X4.U
2490 LABEL "Tc"
2500 !
2510 PEN 0
2520 MOVE X2,Z1
2530 RETURN
2540 ! UPDATE
2550 N=0
2560 IF R=1 OR R MOD 5=0 THEN 25
80
2570 RETURN
2580 W0=W
2590 U0=U
2600 S0=S
2610 RETURN
2620 END
```

ANNEX B

Equivalence of proposed equations for the correction for the thermal resistance of HFT

Fig. B-1 presents the system involved in the demonstration of the theoretical equivalence of the equations proposed by different authors to correct for the thermal resistance of HFTs. The system represents the immersion of a human body segment in water, but it can also be applied in air with consideration for the boundary layer. In this system, $\dot{H}_{corr}$ is the thermal flux ($W \cdot m^{-2}$) through the skin corrected for the insulating effect of the HFT, which corresponds to the true thermal flux through the skin not covered by a HFT. $\dot{H}_{meas}$ is the measured heat flow value ($W \cdot m^{-2}$), T_c is the core temperature of the segment for which the heat flow is measured (°C), T_{sk} is the temperature of the uncovered skin of the segment (°C), T_l is the temperature of the skin under the lower surface of the HFT (°C), T_u is the temperature of the upper surface of the HFT (°C), T_w is the temperature of the water (°C), R_T is the thermal resistance of the HFT ($°C \cdot m^2 \cdot W^{-1}$), R_t is the thermal resistance of the tissue ($°C \cdot m^2 \cdot W^{-1}$), and R_w is the thermal resistance of the water ($°C \cdot m^2 \cdot W^{-1}$).

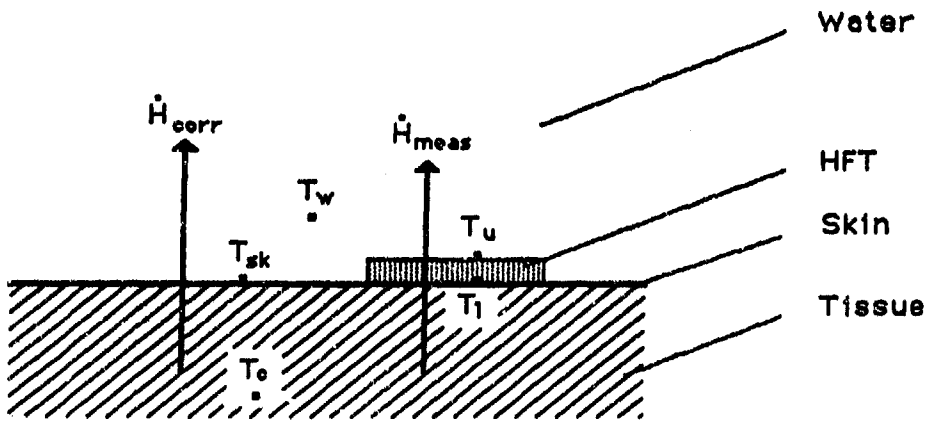

Figure B-1. Schematic representation of the thermal system involved in the demonstration of the theoritical equivalence of the equations proposed by different authors for the correction for the thermal resistance of the HFTs.

From Fourier's law of heat transfer by conduction:

$$\dot{H}_{corr} = \frac{T_c - T_{sk}}{R_t} \quad \text{(B-1)}$$

$$\dot{H}_{corr} = \frac{T_{sk} - T_w}{R_w} \quad \text{(B-2)}$$

$$\dot{H}_{corr} = \frac{T_c - T_w}{R_t - R_w} \quad \text{(B-3)}$$

In addition, $\dot{H}_{meas}$ can be described by:

$$\dot{H}_{meas} = \frac{T_c - T_l}{R_t} \quad \text{(B-4)}$$

$$\dot{H}_{meas} = \frac{T_l - T_u}{R_T} \quad \text{(B-5)}$$

$$\dot{H}_{meas} = \frac{T_u - T_w}{R_w} \quad \text{(B-6)}$$

$$\dot{H}_{meas} = \frac{T_c - T_w}{R_t + R_T + R_w} \quad \text{(B-7)}$$

Knowing that from equation B-5:

$$T_u = T_l - R_T \bullet \dot{H}_{meas} \quad \text{(B-8)}$$

and from equation B-6:

$$R_w = \frac{T_u - T_w}{\dot{H}_{meas}} \tag{B-9}$$

we can now express Eq. B-2 as follows:

$$\dot{H}_{corr} = \frac{(T_{sk} - T_w) \cdot \dot{H}_{meas}}{(T_l - T_w) - R_T \cdot \dot{H}_{meas}} \tag{B-10}$$

Eq. B-10 was proposed by Strong et al. (1985).

From Eq. B-4:

$$R_t = \frac{T_c - T_l}{\dot{H}_{meas}} \tag{B-11}$$

and from Eq. B-5:

$$T_l = T_u + R_T \cdot \dot{H}_{meas} \tag{B-12}$$

Therefore, Eq. B-1 can now be expressed as follows:

$$\dot{H}_{corr} = \frac{(T_c - T_{sk}) \cdot \dot{H}_{meas}}{(T_c - T_l)} \tag{B-13}$$

$$\dot{H}_{corr} = \frac{T_c - T_{sk}}{(T_c - T_u)/\dot{H}_{meas} - R_T} \tag{B-14}$$

Eqs. B-13 and B-14 are simply rearranged forms of the equation of Gin et al. (1980).

From Eqs. B-3 and B-7:

$$\dot{H}_{corr} \cdot (R_t + R_w) = \dot{H}_{meas} \cdot (R_t + R_T + R_w) \tag{B-15}$$

$$\dot{H}_{corr} \cdot (R_t + R_w) = \dot{H}_{meas} \cdot (R_t + R_w) + \dot{H}_{meas} \cdot R_T \tag{B-16}$$

By rearrangement, Eq. B-16 becomes:

$$1 = \frac{\dot{H}_{meas} \cdot (R_t + R_w)}{\dot{H}_{corr} \cdot (R_t + R_w) - \dot{H}_{meas} \cdot R_T} \tag{B-17}$$

$$\dot{H}_{corr} = \frac{\dot{H}_{meas} \cdot \dot{H}_{corr} \cdot (R_t + R_w)}{\dot{H}_{corr} \cdot (R_t + R_w) - \dot{H}_{meas} \cdot R_T} \tag{B-18}$$

By using Eq. B-3, Eq. B-18 can be rearranged and expressed as follows:

$$\dot{H}_{corr} = \frac{\dot{H}_{meas}}{1 - \dot{H}_{meas} \cdot R_T/(T_c - T_w)} \tag{B-19}$$

Eq. B-19 is the correction equation derived by Wissler and Ketch (1982), and later by Sowood (1986).

This mathematical demonstration proves the theoritical equivalence of all the equations proposed by different authors to correct for the thermal resistance of HFTs.

SECURITY CLASSIFICATION OF FORM
(highest classification of Title, Abstract, Keywords)

DOCUMENT CONTROL DATA

(Security classification of title, body of abstract and indexing annotation must be entered when the overall document is classified)

1. ORIGINATOR (the name and address of the organization preparing the document. Organizations for whom the document was prepared, e.g. Establishment sponsoring a contractor's report, or tasking agency, are entered in section 12.)

DCIEM, North York, Ont.

2. DOCUMENT SECURITY CLASSIFICATION (overall security classification of the document, including special warning terms if applicable)

Unclassified

3. DOCUMENT TITLE (the complete document title as indicated on the title page. Its classification should be indicated by the appropriate abbreviation (S,C,R or U) in parentheses after the title.)

Methodology for calibration and use of heat flux transducers

4. DESCRIPTIVE NOTES (the category of the document, e.g. technical report, technical note or memorandum. If appropriate, enter the type of report, e.g. interim, progress, summary, annual or final. Give the inclusive dates when a specific reporting period is covered.)

DCIEM Research Report

5. AUTHOR(S) (Last name, first name, middle initial. If military, show rank, e.g. Doe, Maj. John E.)

Michel B. Ducharme and John Frim

6. DOCUMENT DATE (month and year of publication of document)	7a. NO. OF PAGES (total containing information. Include Annexes, Appendices, etc.)	7b. NO. OF REFS (total cited in document)
	55	13

8a. PROJECT OR GRANT NO. (if appropriate, the applicable research and development project or grant number under which the document was written. Please specify whether project or grant)	8b. CONTRACT NO. (if appropriate, the applicable number under which the document was written)

9a. ORIGINATOR'S DOCUMENT NUMBER (the official document number by which the document is identified by the originating activity. This number must be unique to this document.)	9b. OTHER DOCUMENT NO.(S) (Any other numbers which may be assigned this document either by the originator or by the sponsor)
DCIEM No. 91-45	

10. DOCUMENT AVAILABILITY (any limitations on further dissemination of the document, other than those imposed by security classification)

( ) Unlimited distribution
( ) Distribution limited to defence departments and defence contractors; further distribution only as approved
( ) Distribution limited to defence departments and Canadian defence contractors; further distribution only as approved
( ) Distribution limited to government departments and agencies; further distribution only as approved
( ) Distribution limited to defence departments; further distribution only as approved
( ) Other

11. ANNOUNCEMENT AVAILABILITY (any limitation to the bibliographic announcement of this document. This will normally correspond to the Document Availabilty (10). However, where further distribution (beyond the audience specified in 10) is possible, a wider announcement audience may be selected.)

12. SPONSORING ACTIVITY (the name of the department project office or laboratory sponsoring the research and development. Include the address.)

SAMPLE PRINT OF FORM : DCD03

13. ABSTRACT (a brief and factual summary of the document. It may also appear elsewhere in the body of the document itself. It is highly desirable that the abstract of classified documents be unclassified. Each paragraph of the abstract shall begin with an indication of the security classification of the information in the paragraph (unless the document itself is unclassified) represented as (S), (C), (R), or (U). It is not necessary to include here abstracts in both offical languages unless the text is bilingual).

The direct assessment of heat flux from the body is a basic measurement in thermal physiology. Heat flux transducers (HFTs) are being used increasingly for that purpose under different environmental conditions. However, questions have been raised regarding the accuracy of the manufacturer's constant of calibration, and also about the effect of the thermal resistance of the device on the true thermal flux from the skin. Two different types of waterproofed HFTs were checked for their calibration using the Rapid-k thermal conductivity instrument. A detailed description of the methodology used during the calibration is given. The mean differences between our calibration constants and the manufacturers' constants were +20.2 ± 7.1% (n = 15) for Thermonetics Corporation's HFTs (San Diego, CA) and -0.7 + 4.8% (n = 12) for Concept Engineering's HFTs (Old Saybrook, CT). The highly significant statistical difference in the error of calibration between the two manufacturers ($p < 0.001$) becomes an important criterion for the selection of HFTs.

A model capable of simulating a large range of "tissue" insulation was used to study the effect of the underlying tissue insulation on the relative error in thermal flux due to the thermal resistance of the HFTs. The data show that the deviation from the true value of thermal flux increases with the reciprocal of the underlying tissue insulation ($r = 0.99$, $p < 0.001$). The underestimation of the heat flux through the skin measured by an HFT is minimal when the device is used on vasoconstricted skin in cool subjects (3 to 13% error), but becomes important when used on warm vasodilated subjects (29 to 35% error), and even more important on metallic skin mannequins (> 60% error). In order to optimize the accuracy of the heat flux measurements by HFTs, it is important to recalibrate the HFTs from Thermonetics Corporation, and to correct the heat flux values for the thermal resistance of the HFT when used on vasodilated tissues.

14. KEYWORDS, DESCRIPTORS or IDENTIFIERS (technically meaningful terms or short phrases that characterize a document and could be helpful in cataloguing the document. They should be selected so that no security classification is required. Identifiers, such as equipment model designation, trade name, military project code name, geographic location may also be included. If possible, keywords should be selected from a published thesaurus, e.g. Thesaurus of Engineering and Scientific Terms (TEST) and that thesaurus identified. If it is not possible to select indexing terms which are Unclassified, the classification of each should be indicated as with the title.)

Heat flux transducers, tissue insulation

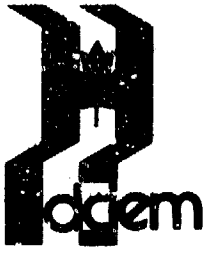

DEFENCE AND CIVIL INSTITUTE OF ENVIRONMENTAL MEDICINE
1133 Sheppard Ave West, PO Box 2000, Downsview, Ontario, Canada
Telephone (416) 635-2000